

Perspectives for Atmospheric Neutrino Studies with Hyper-Kamiokande

Andrew Santos

Laboratoire Leprince-Ringuet
École Polytechnique – IP Paris
MMTE Workshop (5 July 2023)



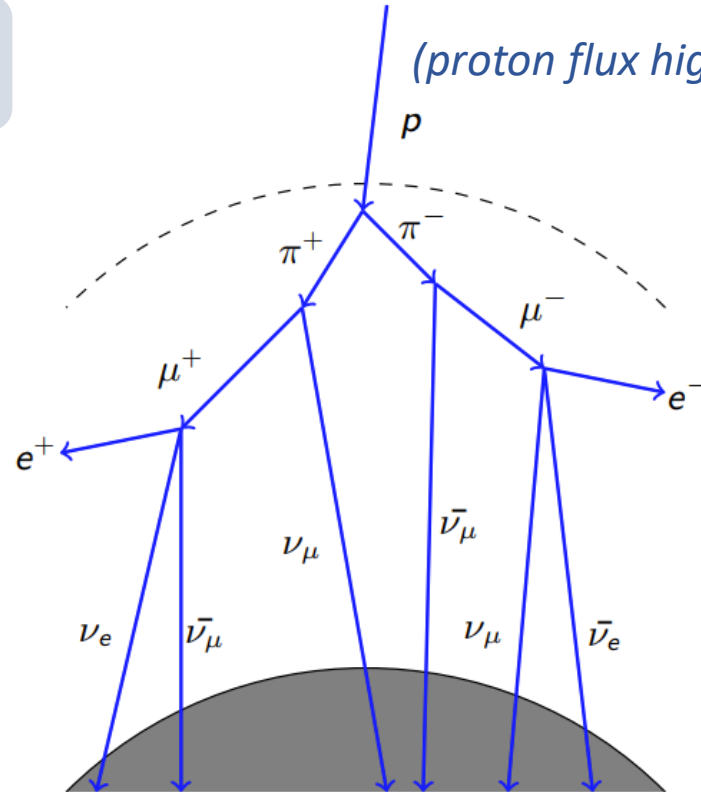
Hyper-Kamiokande



Cosmic ray interactions with the atmosphere create neutrinos.

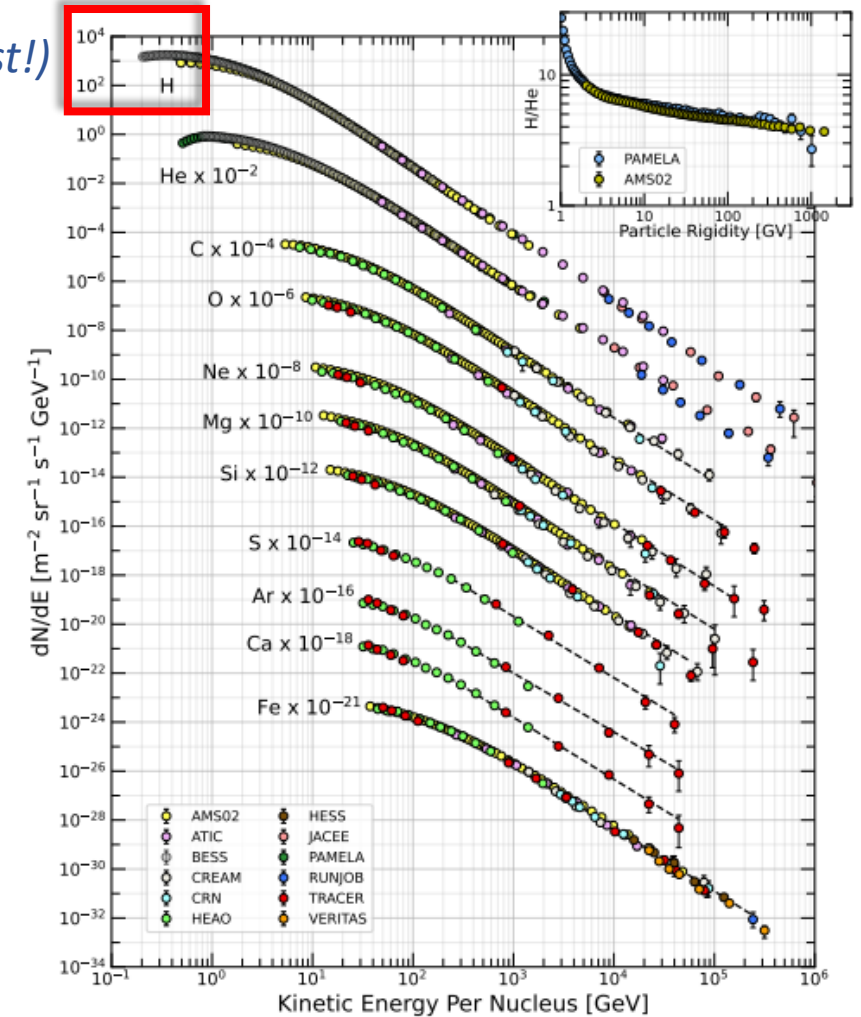
Atmospheric ν production!

- **Primary cosmic rays** interact with nuclei in the Earth's atmosphere.
- Mostly **protons**, they create secondary rays of hadrons and their decays.
- These interactions leave **an abundance of neutrinos!**
- **Difficult to model** these interactions (cosmic ray flux, hadronic interactions, geomagnetic field, etc.)
- Neutrinos **travel** across the Earth between **~ 10 km to ~ 10000 km!**



$$\frac{\phi_{\nu_\mu} + \phi_{\bar{\nu}_\mu}}{\phi_{\nu_e} + \phi_{\bar{\nu}_e}} \simeq 2 \text{ below } 1 \text{ GeV}$$

$$\frac{\phi_{\nu_\mu} + \phi_{\bar{\nu}_\mu}}{\phi_{\nu_e} + \phi_{\bar{\nu}_e}} > 2 \text{ above } 1 \text{ GeV}$$

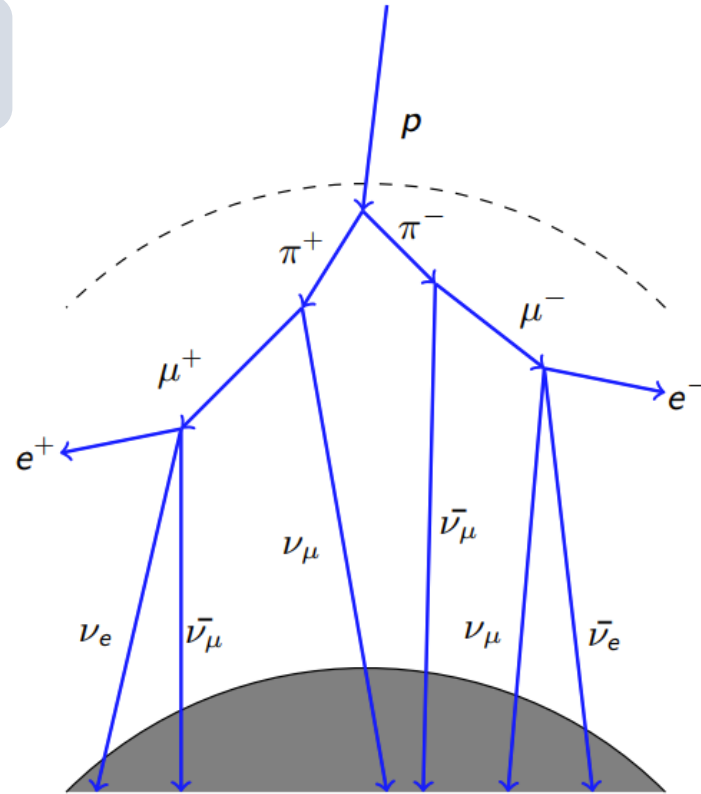


R.L. Workman *et al.* (PDG), Prog. Theor. Exp. Phys., 083C01 (2022)

Atmospheric ν cover a broad range of energies (and distances)!

Atmospheric ν production!

- **Primary cosmic rays** interact with nuclei in the Earth's atmosphere.
- Mostly **protons**, they create secondary rays of hadrons and their decays.
- These interactions leave **an abundance of neutrinos!**
- **Difficult to model** these interactions (cosmic ray flux, hadronic interactions, geomagnetic field, etc.)
- Neutrinos **travel** across the Earth between **~ 10 km to ~ 10000 km!**
- Neutrinos also **oscillate in vacuum and in matter...!**

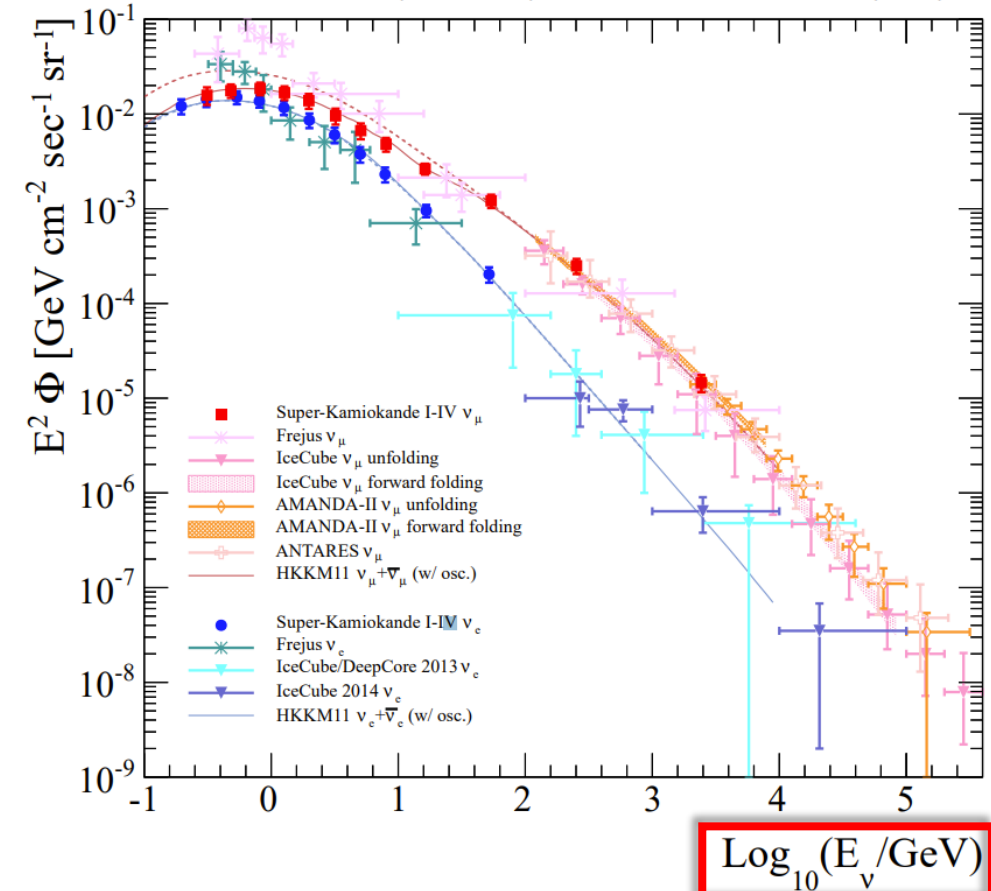


$$\frac{\phi_{\nu_\mu} + \phi_{\bar{\nu}_\mu}}{\phi_{\nu_e} + \phi_{\bar{\nu}_e}} \simeq 2 \text{ below } 1 \text{ GeV}$$

$$\frac{\phi_{\nu_\mu} + \phi_{\bar{\nu}_\mu}}{\phi_{\nu_e} + \phi_{\bar{\nu}_e}} > 2 \text{ above } 1 \text{ GeV}$$

(several orders of magnitude in energy!)

E. Richard et al. (SK collab.) Phys. Rev. D 94, 052001 (2016)



Neutrino oscillations are a probe for interesting physics.

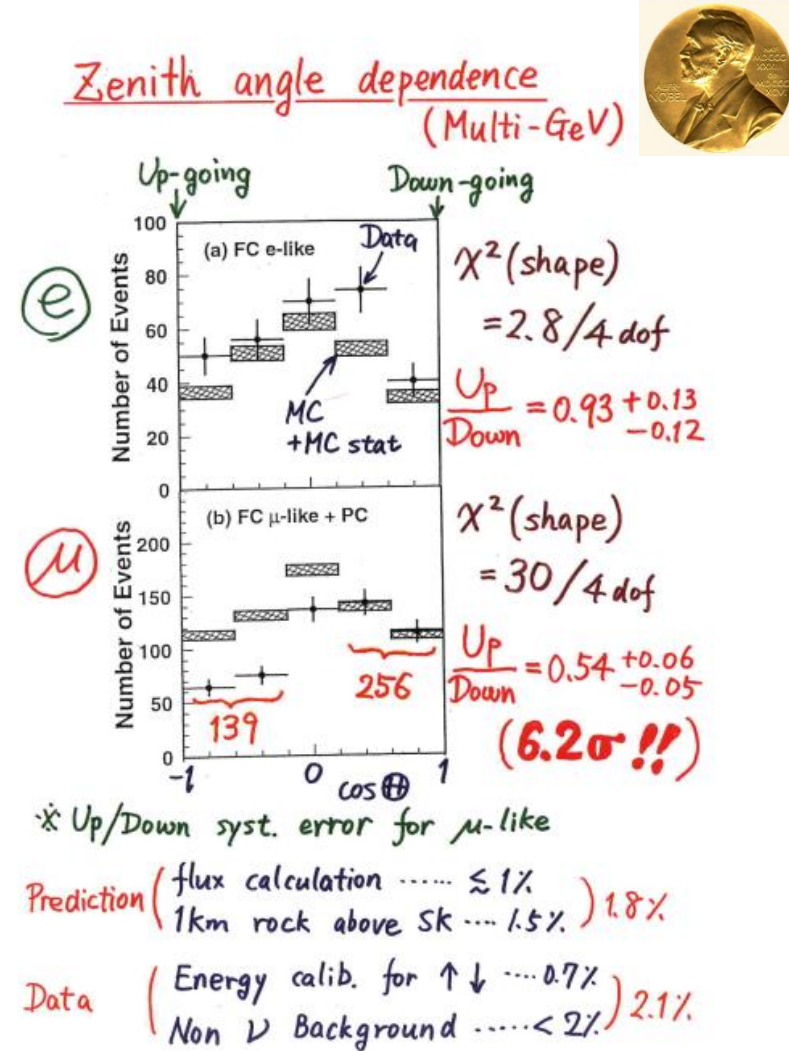
$$\begin{pmatrix} \nu_e \\ \nu_\mu \\ \nu_\tau \end{pmatrix} = U_{\text{PMNS}} \begin{pmatrix} \nu_1 \\ \nu_2 \\ \nu_3 \end{pmatrix}$$

flavour
"interaction"
mass
"propagation"

- Super-Kamiokande (1998) and SNO (2001) experiments find that **neutrinos oscillate**.
- **Fewer ν_μ coming from the ground than expected** (i.e., they changed flavor while traversing the Earth)!
- Then, neutrinos have (differing) masses! **A Nobel Prize...!**

$$U_{\text{PMNS}} = \begin{pmatrix} 1 & 0 & 0 \\ 0 & \cos \theta_{23} & \sin \theta_{23} \\ 0 & -\sin \theta_{23} & \cos \theta_{23} \end{pmatrix} \begin{pmatrix} \cos \theta_{13} & 0 & e^{-i\delta} \sin \theta_{13} \\ 0 & 1 & 0 \\ -e^{+i\delta} \sin \theta_{13} & 0 & \cos \theta_{13} \end{pmatrix} \begin{pmatrix} \cos \theta_{12} & \sin \theta_{12} & 0 \\ -\sin \theta_{12} & \cos \theta_{12} & 0 \\ 0 & 0 & 1 \end{pmatrix}$$

atmospheric Δm_{31}^2
accelerators
solar Δm_{21}^2
reactors



(Pontecorvo-Maki-Nakagawa-Sakata)

Vacuum oscillations probe mixing angles θ and $|\Delta m^2|$.

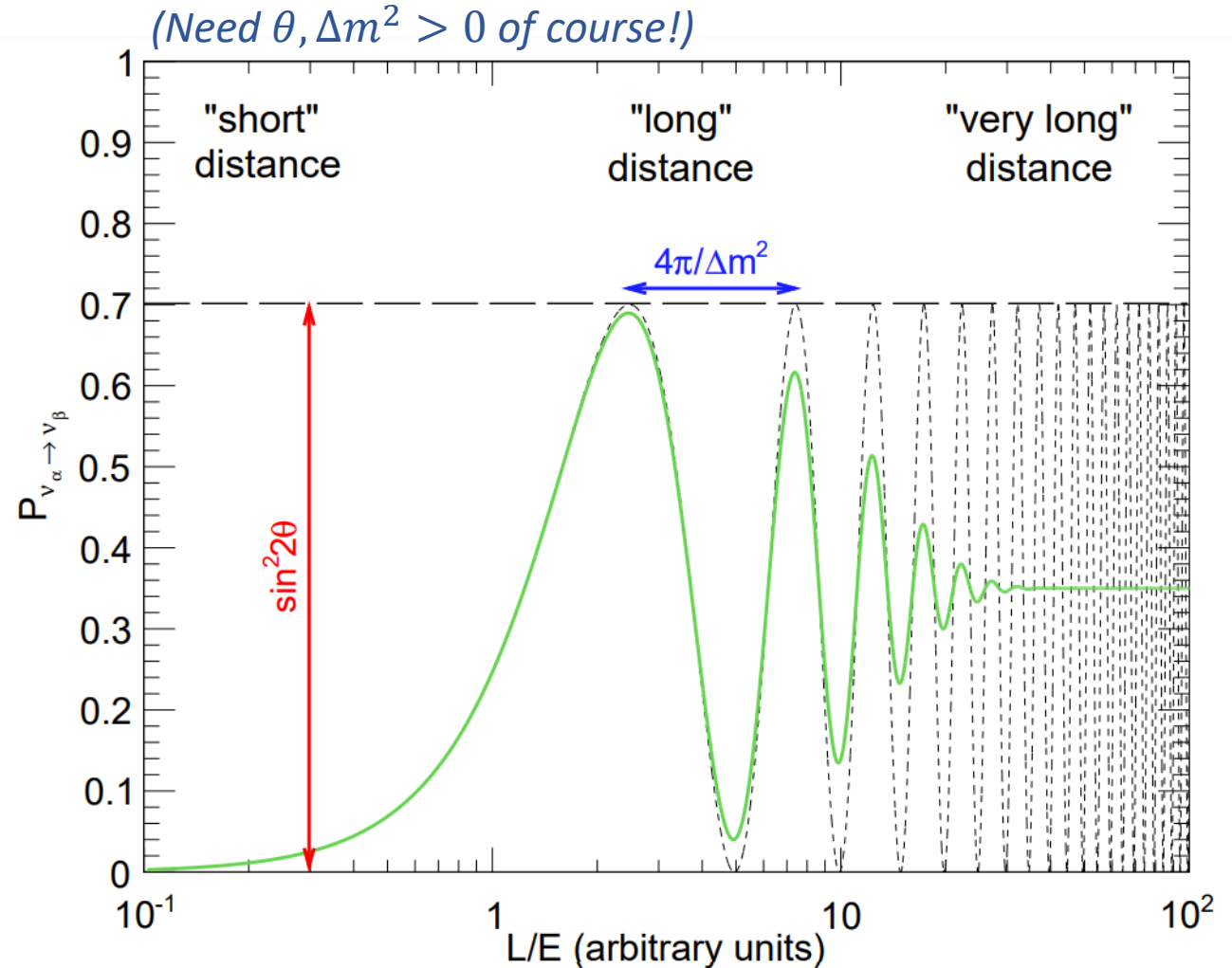
Two-flavor approximation in vacuum

$$\Delta m^2 \equiv m_2^2 - m_1^2$$
$$P(\nu_\alpha \rightarrow \nu_\beta)(L, E) = \sin^2 2\theta \sin^2 \left(\frac{\Delta m^2 L}{4E} \right)$$
$$\approx \sin^2 2\theta \sin^2 \left(1.3 \frac{\Delta m^2 [\text{eV}^2] L [\text{km}]}{E [\text{GeV}]} \right)$$

$$\frac{E [\text{GeV}]}{L [\text{km}]} \sim 10^{-3} \sim \Delta m_{31}^2$$

(setup like T2K experiment!)

- **Accelerator experiments** (e.g., $E \sim 0.6$ GeV, $L \sim 300$ km for T2K/HK) are **designed** to sit at L/E where the effects of Δm_{31}^2 are probed!



Here are two open questions for neutrino physics.

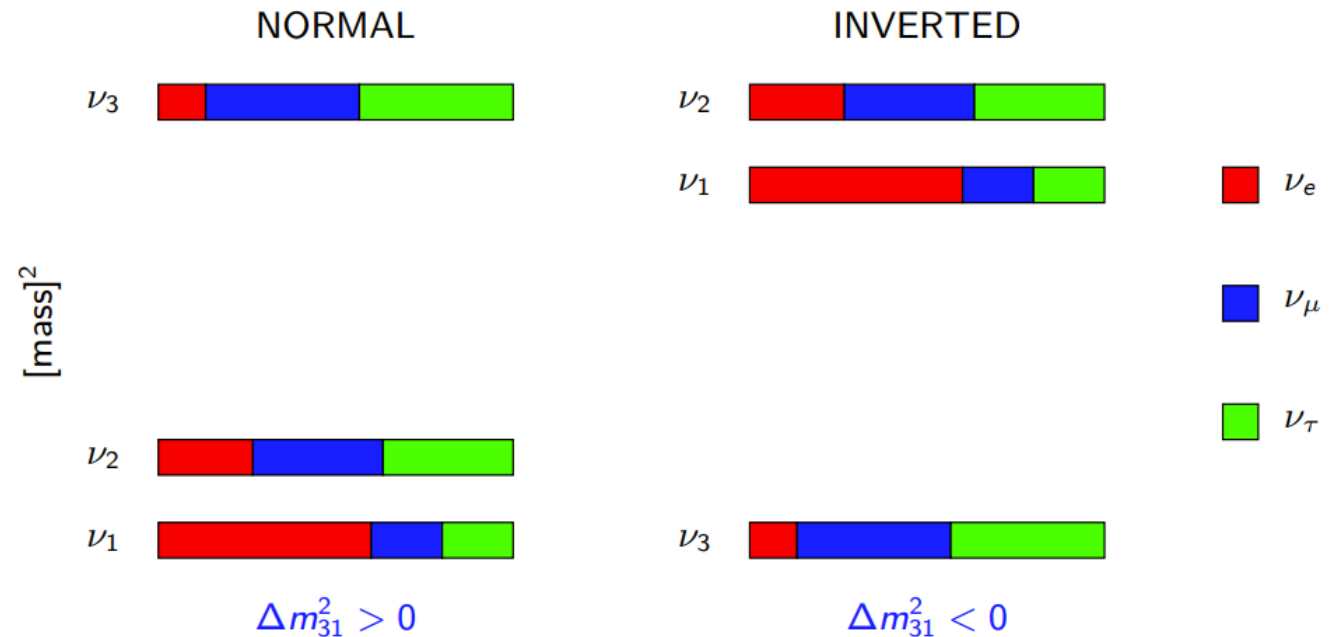
Charge-Parity (CP) Violation

$$\delta_{CP} \neq 0 \Rightarrow P(\nu_\alpha \rightarrow \nu_\beta) \neq P(\bar{\nu}_\alpha \rightarrow \bar{\nu}_\beta)$$

(maximal CPV, leptogenesis...?)

Mass Hierarchy (MH)/Ordering (MO)

$$\Delta m_{21}^2 > 0 \text{ but what about } \Delta m_{31}^2?$$



$$\begin{pmatrix} \nu_e \\ \nu_\mu \\ \nu_\tau \end{pmatrix} = U_{\text{PMNS}} \begin{pmatrix} \nu_1 \\ \nu_2 \\ \nu_3 \end{pmatrix}$$

flavour "interaction" mass "propagation"

$$U_{\text{PMNS}} = \begin{pmatrix} 1 & 0 & 0 \\ 0 & \cos \theta_{23} & \sin \theta_{23} \\ 0 & -\sin \theta_{23} & \cos \theta_{23} \end{pmatrix} \begin{pmatrix} \cos \theta_{13} & 0 & e^{-i\delta} \sin \theta_{13} \\ 0 & 1 & 0 \\ -e^{+i\delta} \sin \theta_{13} & 0 & \cos \theta_{13} \end{pmatrix} \begin{pmatrix} \cos \theta_{12} & \sin \theta_{12} & 0 \\ -\sin \theta_{12} & \cos \theta_{12} & 0 \\ 0 & 0 & 1 \end{pmatrix}$$

atmospheric Δm_{31}^2 solar Δm_{21}^2

accelerators

reactors

Oscillations in matter are modified by the MSW effect.

$$n_{e,res} \propto \frac{1}{E_\nu} \Delta m_{31}^2 \cos 2\theta_{13}$$

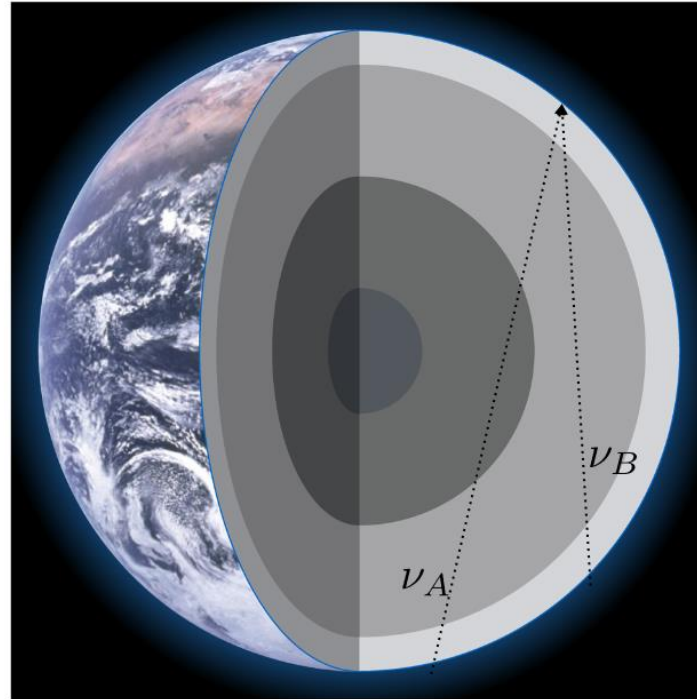
MSW resonance features

- The higher the energy, the **lower the resonant density** required.
- The higher the difference in (squared mass), the **higher the density**.
- The higher the mixing (maximum at $\theta_{13} = 45^\circ$), the **lower the density**.

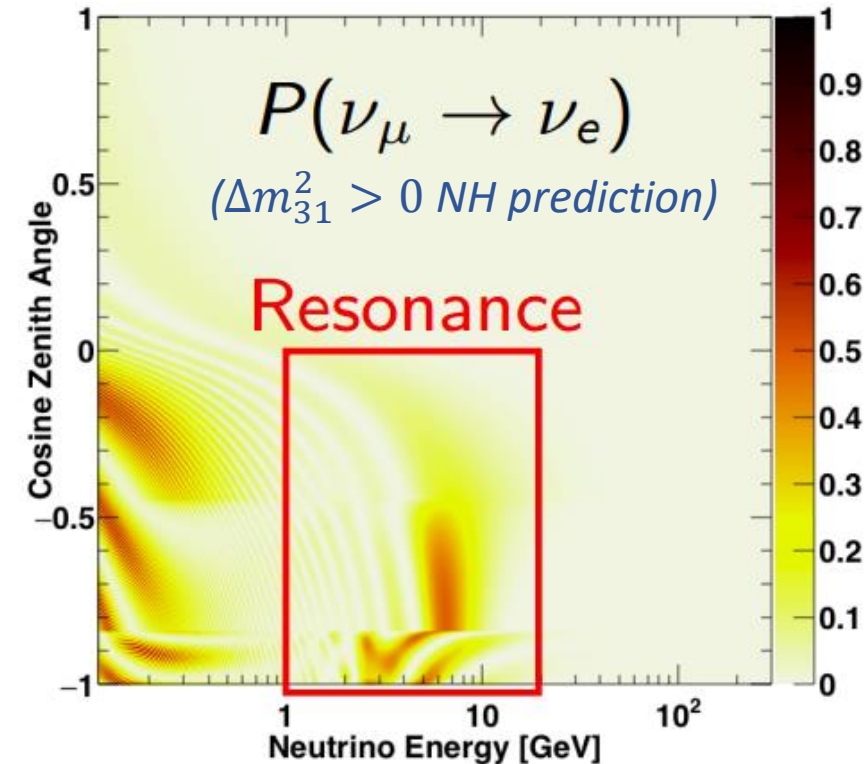
Important sign changes!

- **Change signs** for ν to $\bar{\nu}$.
- Δm_{31}^2 sign depends on mass hierarchy.

(Mikheyev-Smirnov-Wolfenstein effect) $V_{matter} = \sqrt{2}G_F n_e$ for ν_e
 (leads to resonant flavor conversion!)



(we know that $\Delta m_{21}^2 > 0$ from MSW in the sun for ν_e and not $\bar{\nu}_e$!)

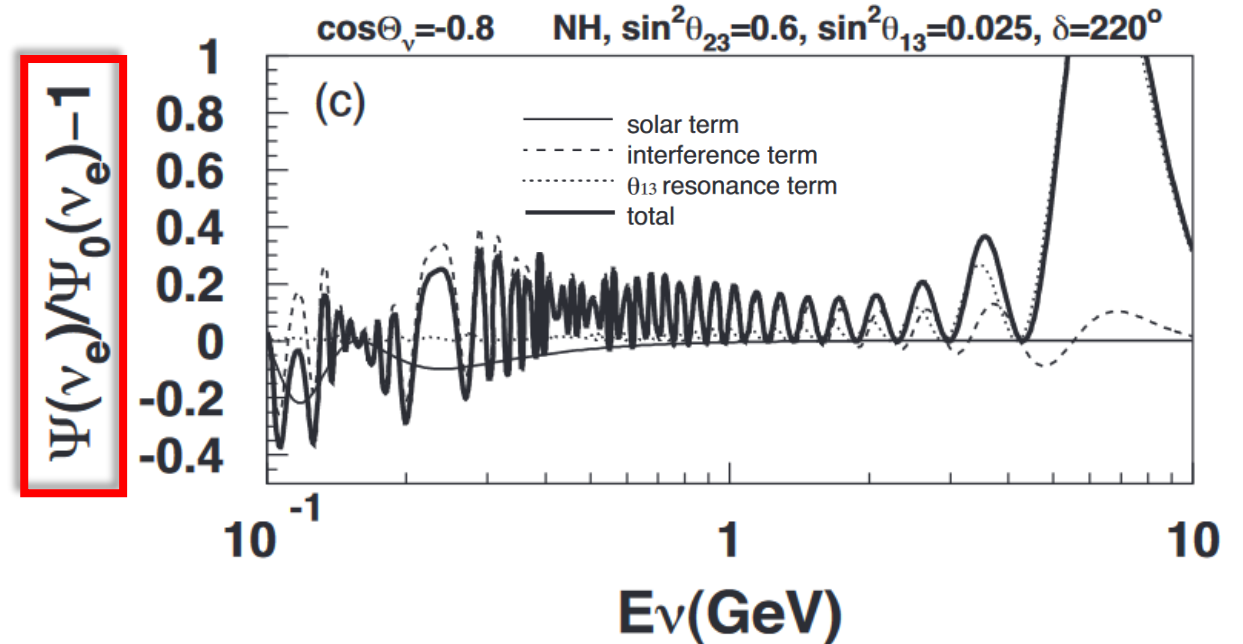


Phys. Rev. D 97, 072001 (2018)

Atmospheric neutrino oscillations can probe δ_{CP} , $\text{sign}(\Delta m_{31}^2)$.

ν_e flux from vacuum/matter oscillations

- P_2 is calculated for Δm_{21}^2 (solar) oscillations
- r is the ratio of ν_μ to ν_e detected (~ 2 at 1 GeV)
- R_2, I_2 are amplitudes for CP-even,-odd
- $\tilde{\theta}$ are effective mixing angles modified by MSW



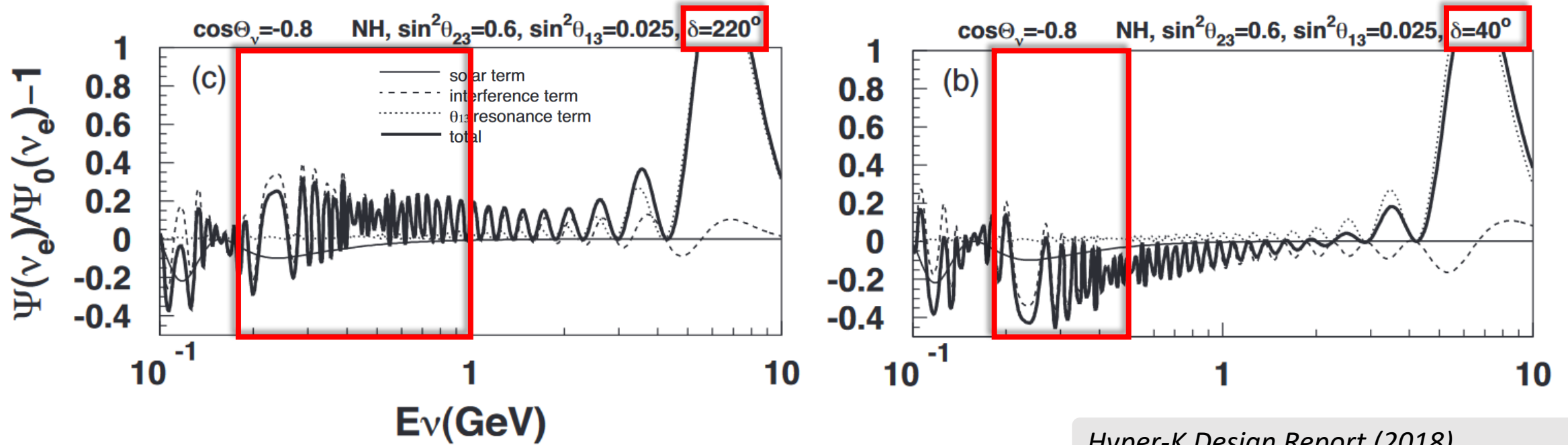
$$\frac{\Psi(\nu_e)}{\Psi_0(\nu_e)} - 1 \approx P_2 \cdot (r \cdot \cos^2 \theta_{23} - 1) \quad (\text{solar term})$$

$$-r \cdot \sin \tilde{\theta}_{13} \cdot \cos^2 \tilde{\theta}_{13} \cdot \sin 2\theta_{23} \cdot (\cos \delta \cdot R_2 - \sin \delta \cdot I_2) \quad (\text{interference term})$$

$$+2 \sin^2 \tilde{\theta}_{13} \cdot (r \cdot \sin^2 \theta_{23} - 1) \quad (\text{resonance term})$$

Hyper-K Design Report (2018)

Sensitivity to δ_{CP} is more present at sub-GeV energies.



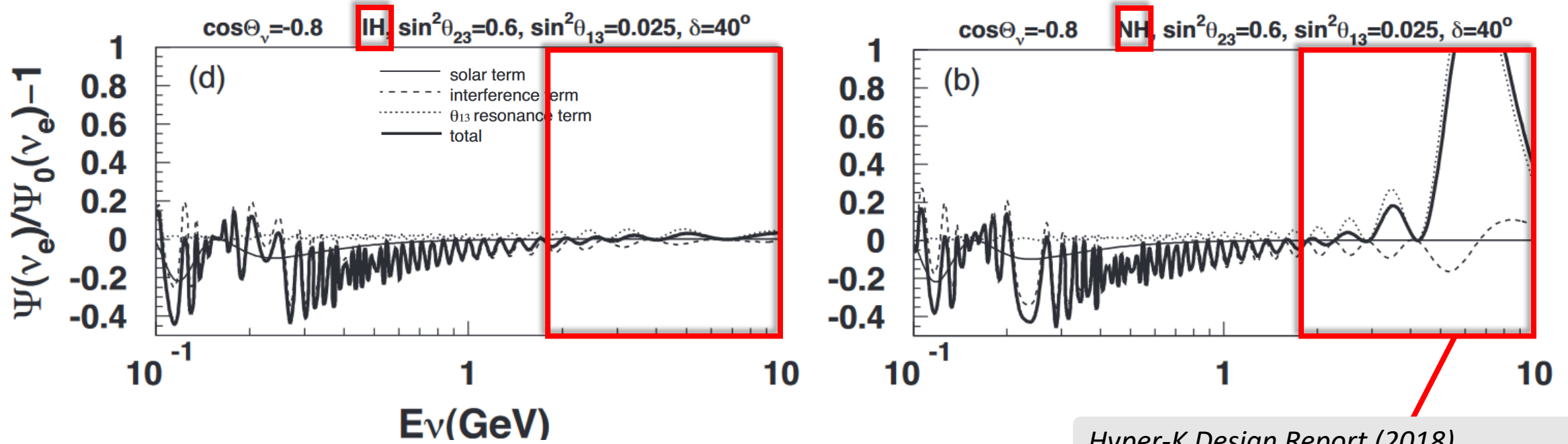
Hyper-K Design Report (2018)

$$\frac{\Psi(\nu_e)}{\Psi_0(\nu_e)} - 1 \approx P_2 \cdot (r \cdot \cos^2 \theta_{23} - 1)$$

$$- r \cdot \sin \tilde{\theta}_{13} \cdot \cos^2 \tilde{\theta}_{13} \cdot \sin 2\theta_{23} \cdot (\cos \delta \cdot R_2 - \sin \delta \cdot I_2) \quad (\text{interference term})$$

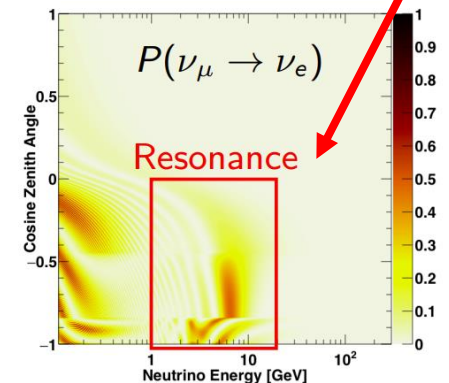
$$+ 2 \sin^2 \tilde{\theta}_{13} \cdot (r \cdot \sin^2 \theta_{23} - 1)$$

Sensitivity to MH is more present at GeV energies.



$$\frac{\Psi(\nu_e)}{\Psi_0(\nu_e)} - 1 \approx P_2 \cdot (r \cdot \cos^2 \theta_{23} - 1) - r \cdot \sin \tilde{\theta}_{13} \cdot \cos^2 \tilde{\theta}_{13} \cdot \sin 2\theta_{23} \cdot (\cos \delta \cdot R_2 - \sin \delta \cdot I_2) + 2 \sin^2 \tilde{\theta}_{13} \cdot (r \cdot \sin^2 \theta_{23} - 1) \quad (\text{resonance term})$$

Hyper-K Design Report (2018)



So, let's study atmospheric ν_e at both sub-GeV and multi-GeV energies!

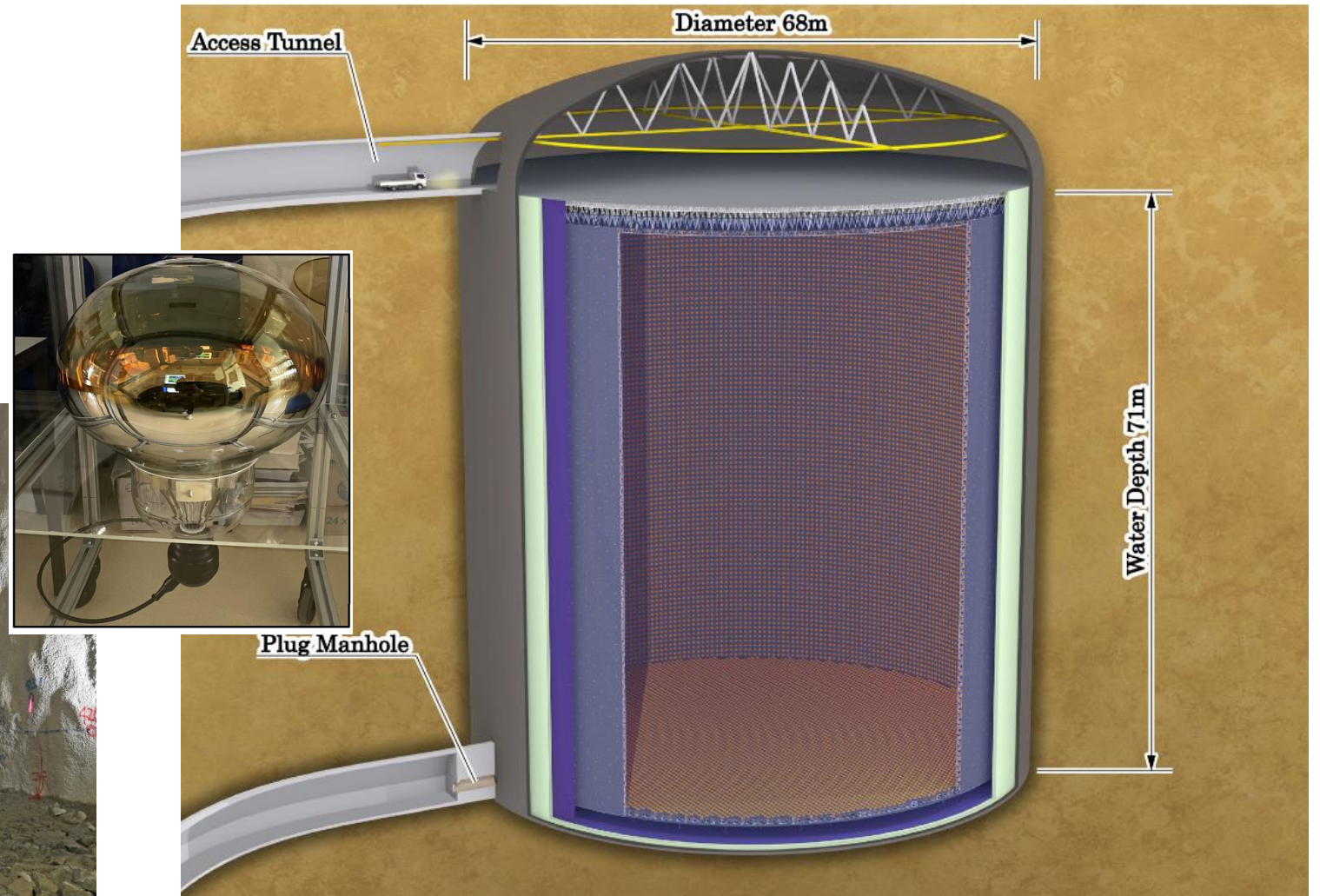
Hyper-K is a next-generation water Cherenkov detector.

- Water Cherenkov detector set to take data **starting in 2027!**
- 20,000 **PMTs** and 1,000 “**multi-PMTs**” (more information on light directionality)
- Total **volume 260kt** with fiducial volume of 190 kt (**~8X bigger than that of Super-K!**)
- Underground to **shield from cosmic ray muons** and still **off-axis for T2K neutrino beam!**

Courtesy of Hyper-K collaboration



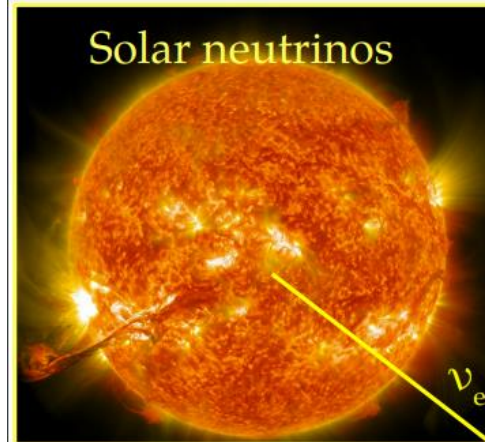
(cavern status last summer!)



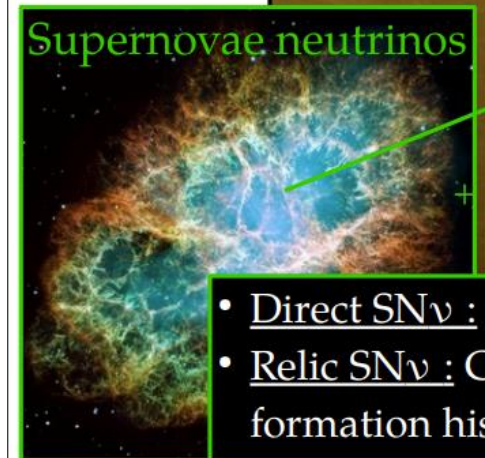
Hyper-K has a multi-faceted physics program.

δ_{CP} and ν MH/MO

- High energy **atmospheric and accelerator neutrinos** are combined.
- There is **complementarity in the energies and distances** covered from these two sources.



- MSW effect in the Sun
- Non-standard interactions in the Sun.

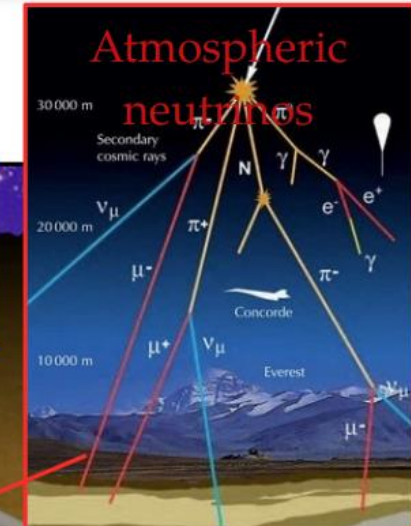
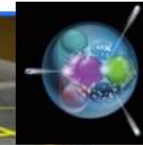


- Direct SN ν : Constrains SN models.
- Relic SN ν : Constrains cosmic star formation history

Physics case

Proton decay

Probe Grand Unified Theories through p-decay (world best sensitivity)



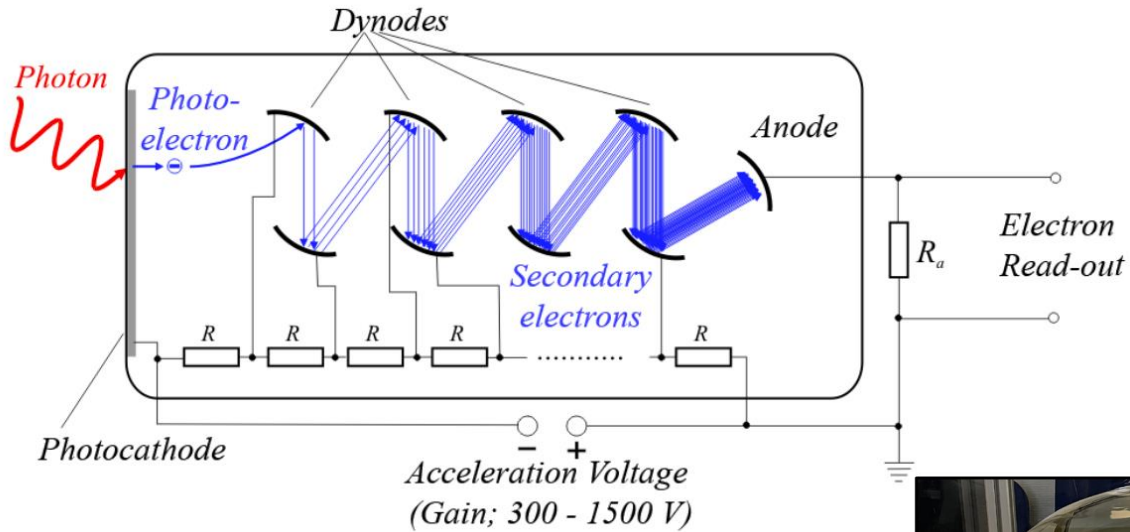
- Observe CP violation for leptons at 5σ
- Precise measurement of δ_{CP} .
- High sensitivity to ν mass ordering.



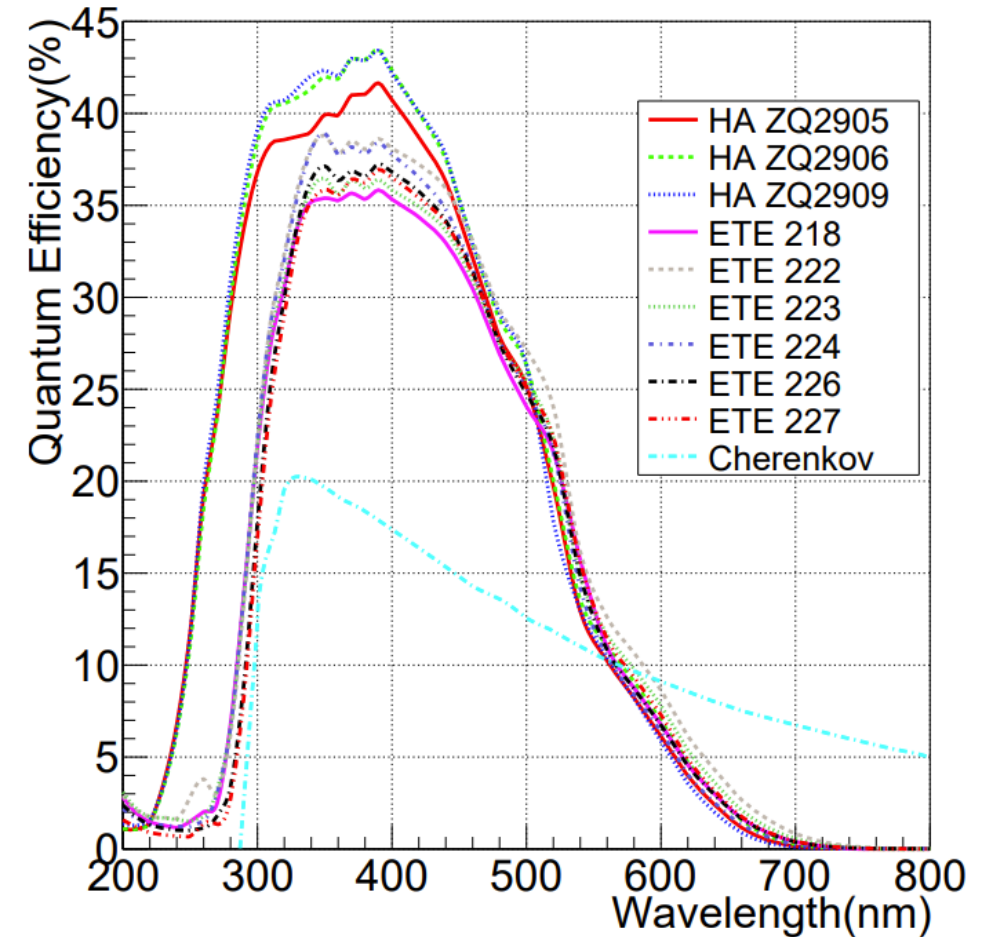
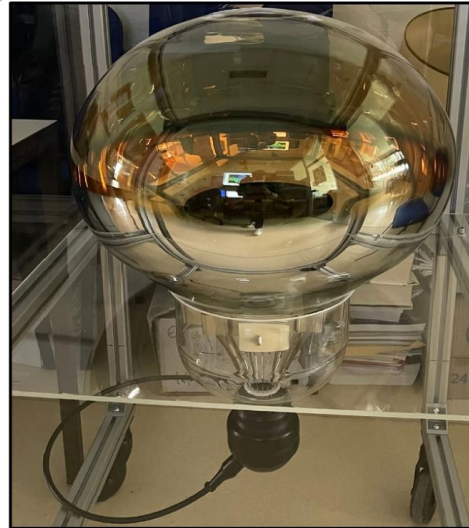
JPARC accelerator neutrinos

Slide from B. Quilain

Photomultiplier tubes are sensitive to Cherenkov radiation.

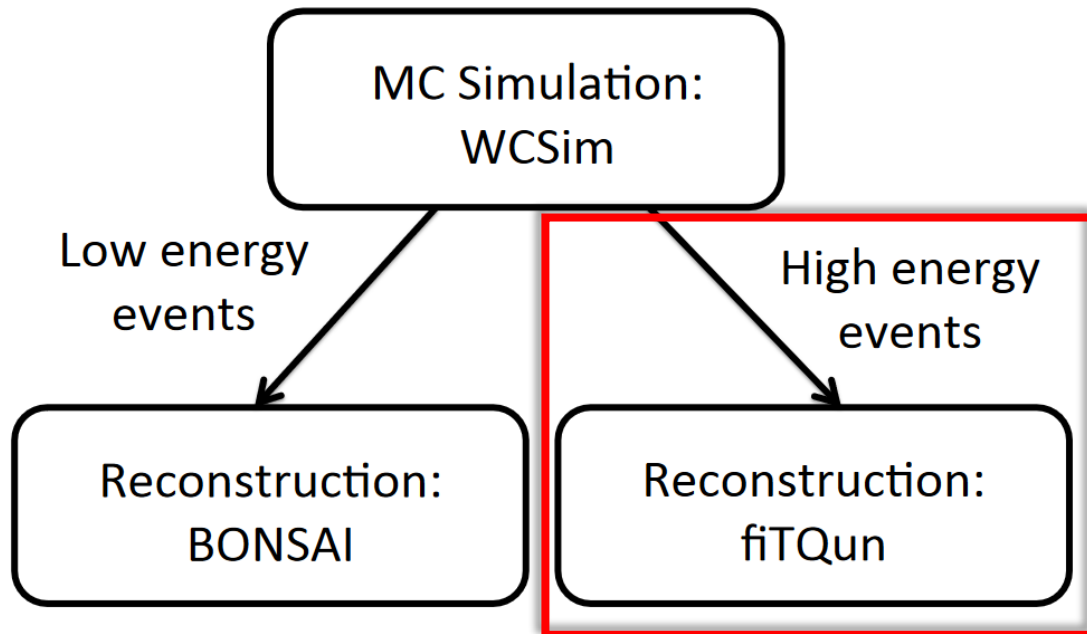


- **Single photons can eject photo-electrons** from photocathode on PMT.
- **Cascade of secondary electrons** are created by the dynodes.
- PMTs are **sensitive to extremely weak light** signatures.



T. Toyama *et al.* (CTA consort.) arXiv:1307.5463 [astro-ph.IM] (2013)

Overview of Super-K reconstruction to be adapted for Hyper-K



- We have access to PMT hit **charge deposited**, **timing**, and **position**.
- We are at **percent-level precision** for reconstructed position, direction, and momentum **at the GeV scale!**

Reconstruction	fiTQun	APFit
True CCQE ν_e sample		
Vertex Resolution	20.6 cm	24.9 cm
Direction Resolution	1.48°	1.68°
Momentum Bias	0.43%	0.63%
Momentum Resolution	2.90%	3.56%
Mis-PID rate	0.02%	0.50%
True CCQE ν_μ sample		
Vertex Resolution	15.8 cm	17.3 cm
Direction Resolution	1.00°	1.28°
Momentum Bias	-0.18%	0.54%
Momentum Resolution	2.26%	2.60%
Mis-PID rate	0.05%	0.91%

(performance at 1 GeV, fully-contained events)

M. Jiang (2019), PhD Thesis, Kyoto University

Atmospheric ν event selection uses inner/outer detectors.

(We want sub-to-multi GeV ν_e !)

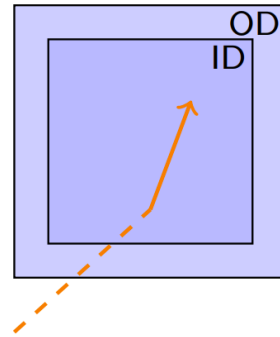
ID/OD event topology

- Fully contained events have better reconstruction.

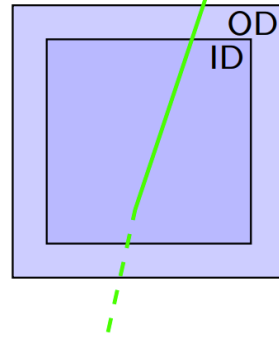
Ring topology for e/μ

Separators for $\nu/\bar{\nu}$

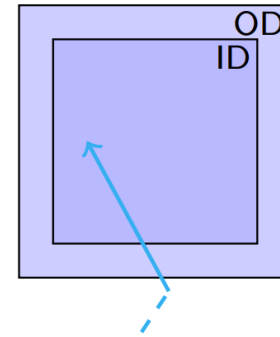
Fully Contained



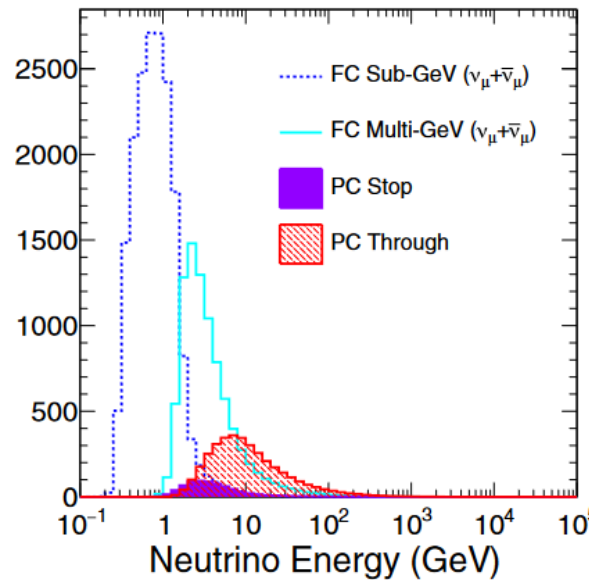
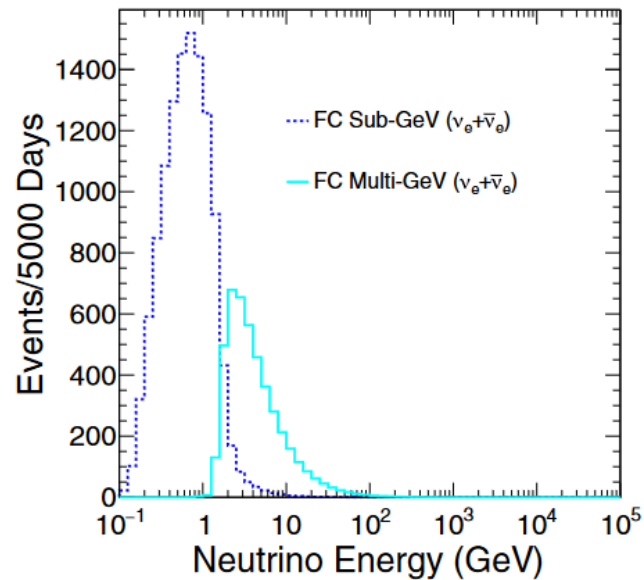
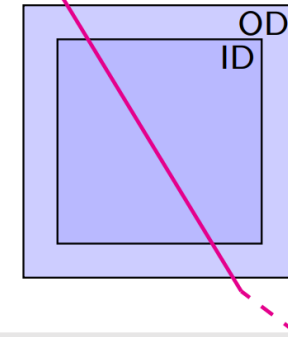
Partially Contained



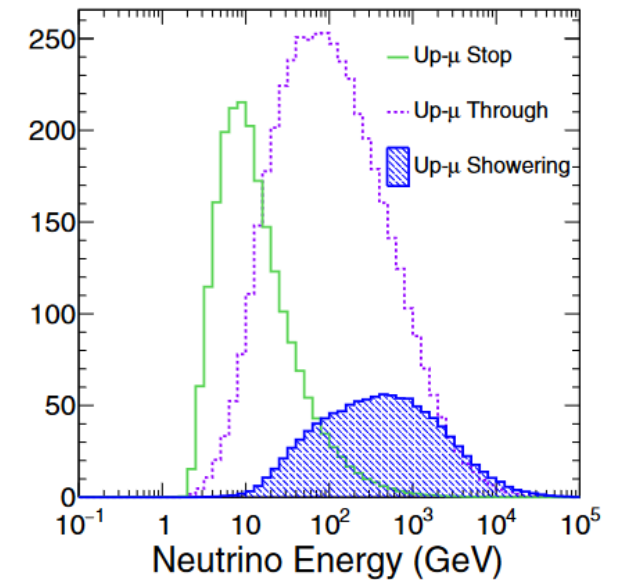
Upward stopping μ



Upward through-going μ



Phys. Rev. D 97, 072001 (2018)



Cherenkov ring properties distinguish between μ and e flavors.

(We want sub-to-multi GeV ν_e !)

ID/OD event topology

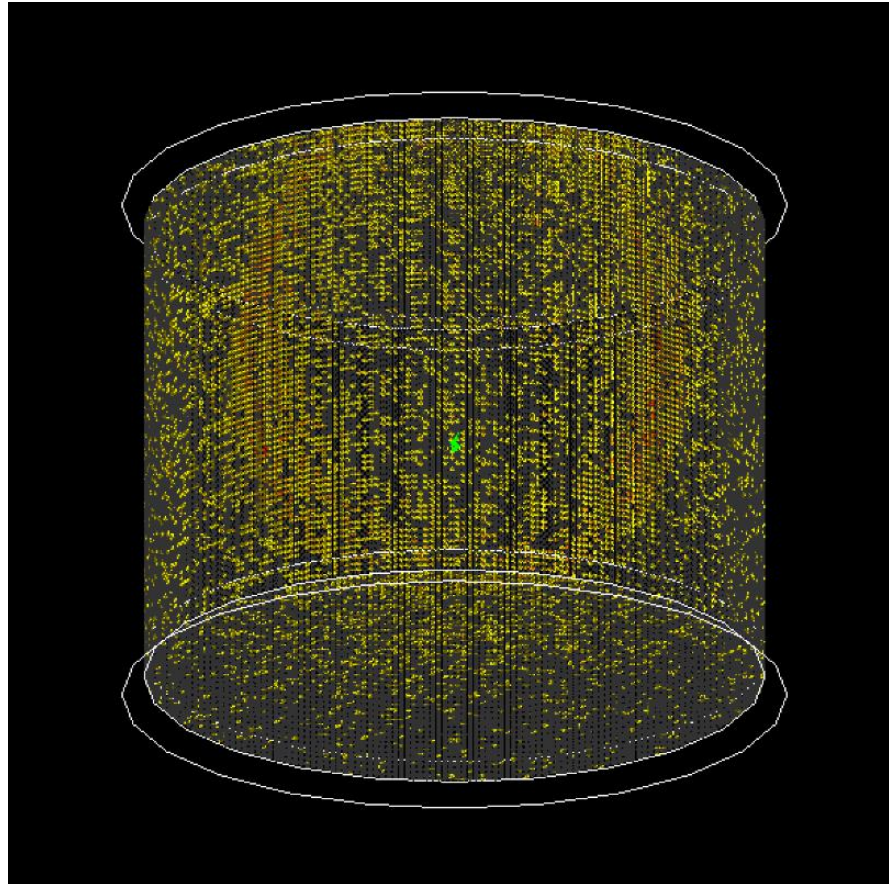
- Fully contained events have better reconstruction.

Ring topology for e/μ

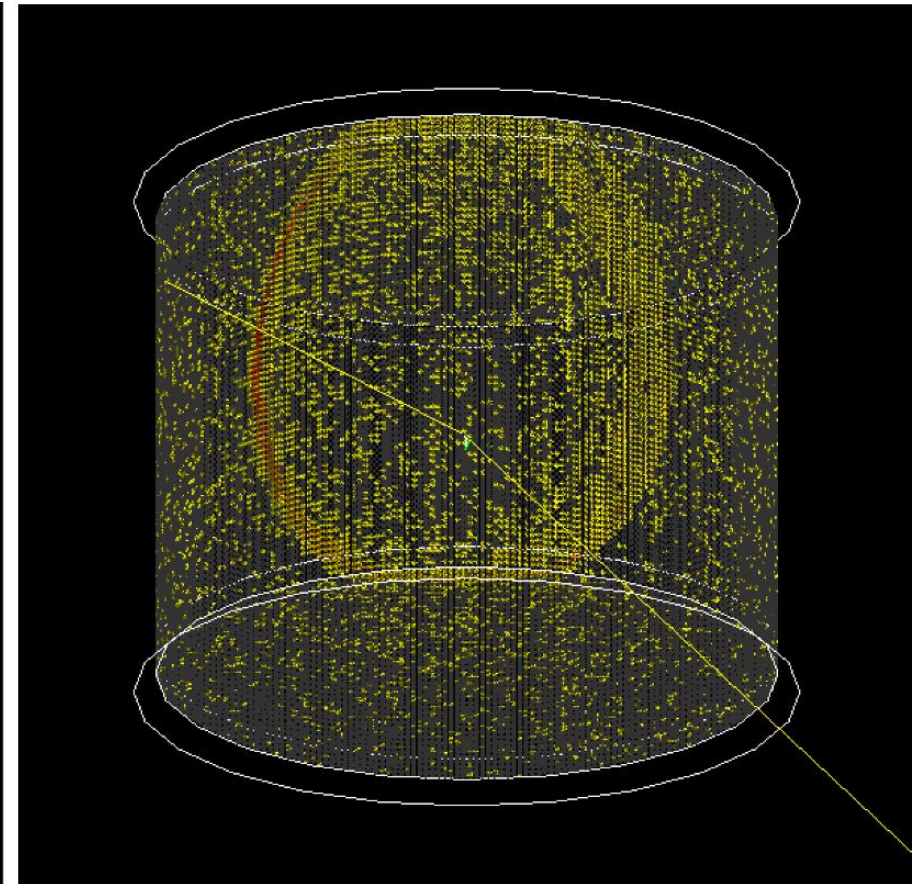
- Muons create sharper rings than electrons.

Separators for $\nu/\bar{\nu}$

(e -like event)



(μ -like event)



Hyper-K Design Report (2018)

Cherenkov ring properties distinguish between μ and e flavors.

(We want sub-to-multi GeV ν_e !)

ID/OD event topology

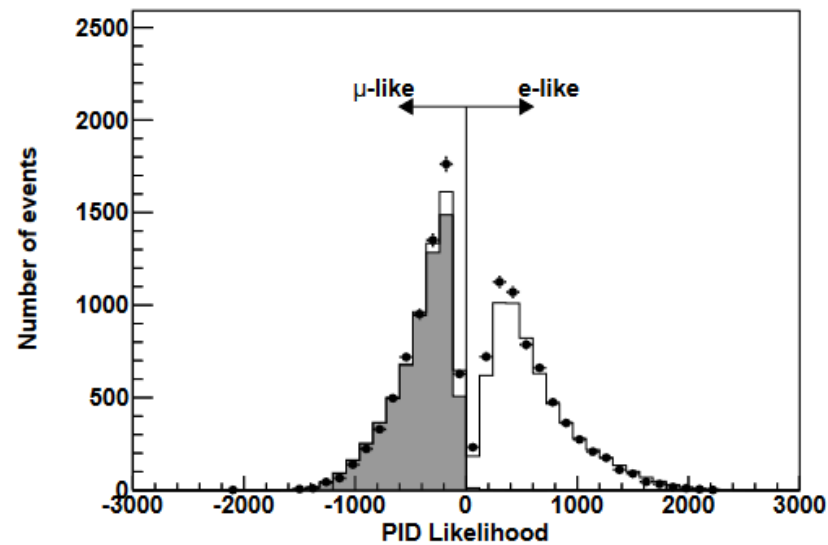
- Fully contained events have better reconstruction.

Ring topology for e/μ

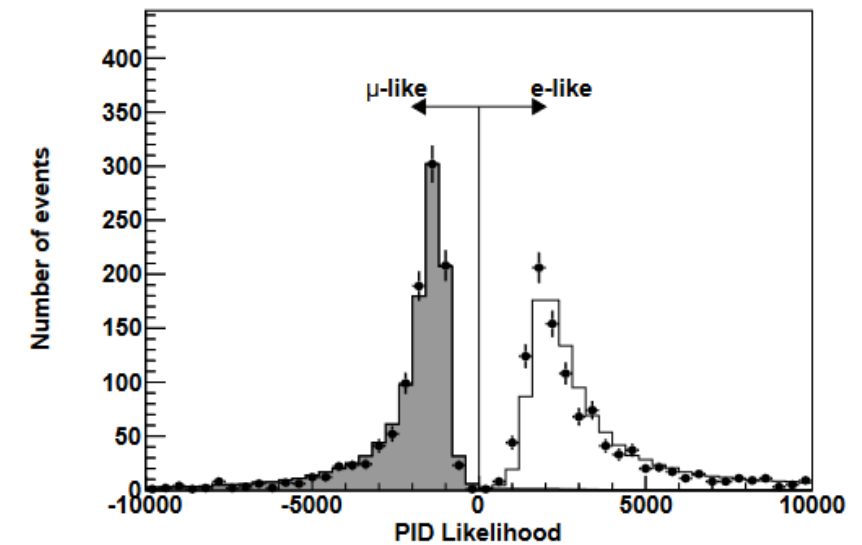
- Muons create sharper rings than electrons.

Separators for $\nu/\bar{\nu}$

(FC sub-GeV event)



(FC GeV event)



M. Jiang (2019), PhD Thesis, Kyoto University

Cherenkov ring properties distinguish between μ and e flavors.

(We want sub-to-multi GeV ν_e !)

ID/OD event topology

- Fully contained events have better reconstruction.

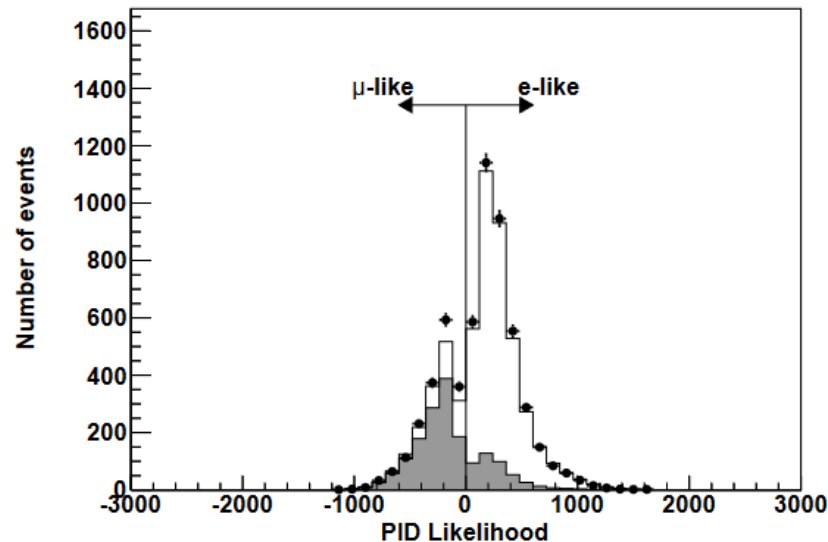
Ring topology for e/μ

- Muons create sharper rings than electrons.

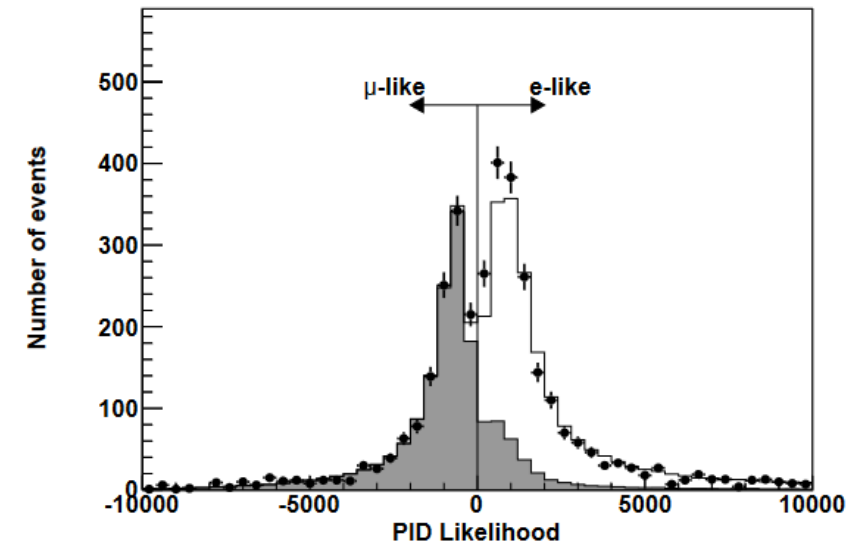
Separators for $\nu/\bar{\nu}$

(but gets more complicated with multi-rings!)

(FC sub-GeV event)



(FC GeV event)



M. Jiang (2019), PhD Thesis, Kyoto University

Three factors determine a likelihood for $\nu/\bar{\nu}$ separation.

(We want sub-to-multi GeV ν_e !)

ID/OD event topology

- Fully contained events have better reconstruction.

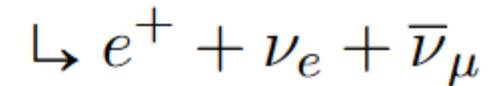
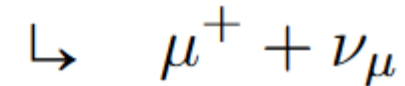
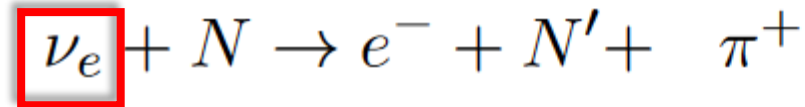
Ring topology for e/μ

- Muons create sharper rings than electrons.

Separators for $\nu/\bar{\nu}$

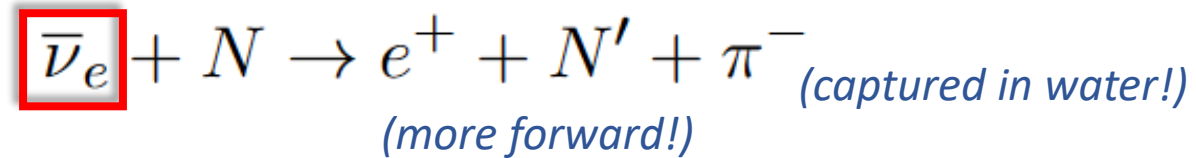
- Number of rings, number of decay- e , transverse momentum

(CC ν_e interactions)



(more particles in the end!)

(CC $\bar{\nu}_e$ interactions)



Three factors determine a likelihood for $\nu/\bar{\nu}$ separation.

(We want sub-to-multi GeV ν_e !)

ID/OD event topology

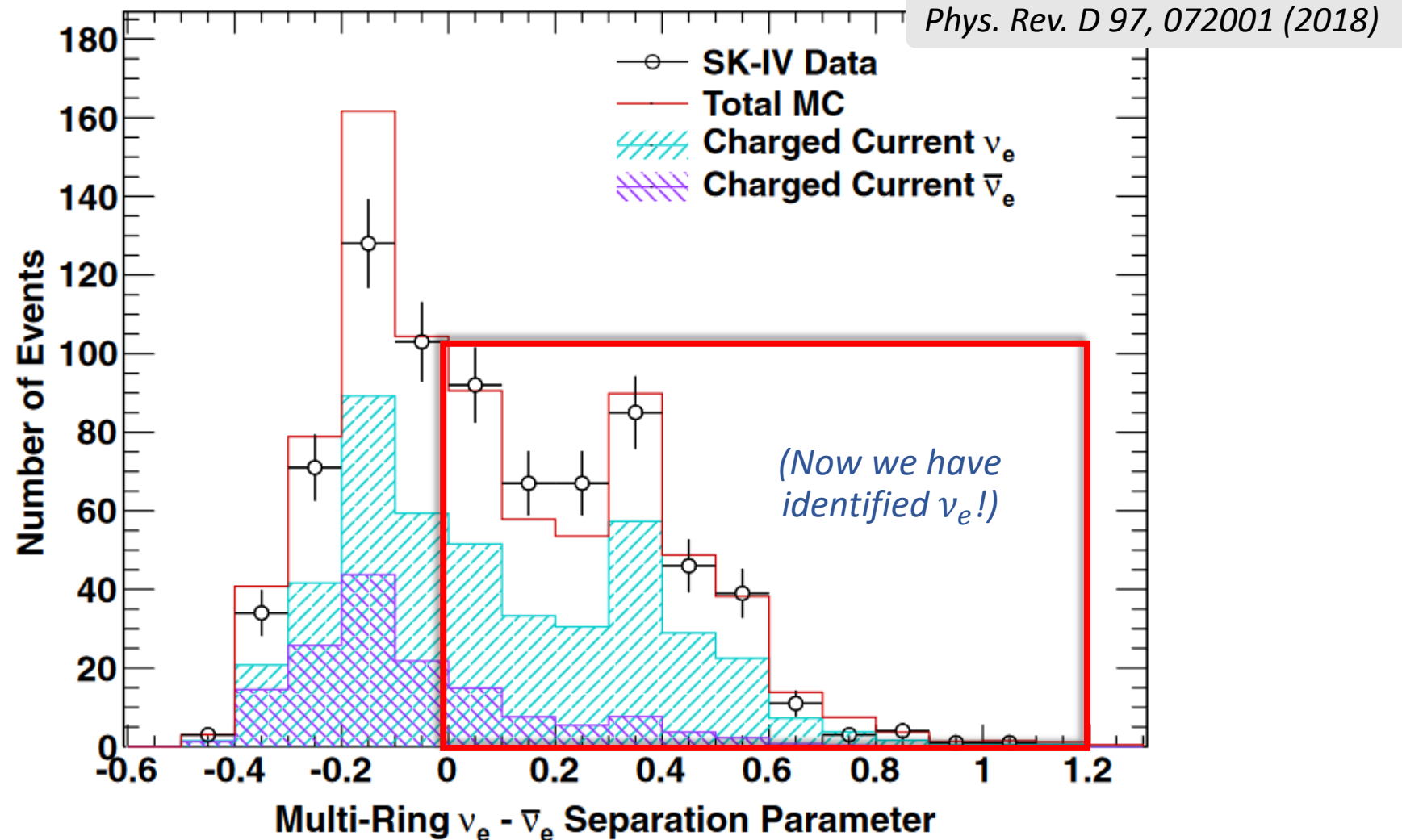
- Fully contained events have better reconstruction.

Ring topology for e/μ

- Muons create sharper rings than electrons.

Separators for $\nu/\bar{\nu}$

- Number of rings, number of decay- e , transverse momentum



Here are the final samples for the sub-to-multi GeV ν_e !

Sample	Energy bins	$\cos \theta_z$ bins	CC ν_e	CC $\bar{\nu}_e$	CC $\nu_\mu + \bar{\nu}_\mu$	CC ν_τ	NC	Data	MC
<i>Fully Contained (FC) Sub-GeV</i>									
e-like, Single-ring									
0 decay-e	5 e^\pm momentum	10 in $[-1, 1]$	0.717	0.248	0.002	0.000	0.033	10294	10266.1
1 decay-e	5 e^\pm momentum	single bin	0.805	0.019	0.108	0.001	0.067	1174	1150.7
μ -like, Single-ring									
0 decay-e	5 μ^\pm momentum	10 in $[-1, 1]$	0.041	0.013	0.759	0.001	0.186	2843	2824.3
1 decay-e	5 μ^\pm momentum	10 in $[-1, 1]$	0.001	0.000	0.972	0.000	0.027	8011	8008.7
2 decay-e	5 μ^\pm momentum	single bin	0.000	0.000	0.979	0.001	0.020	687	687.0
π^0 -like									
Single-ring	5 e^\pm momentum	single bin	0.096	0.033	0.015	0.000	0.856	578	571.8
Two-ring	5 π^0 momentum	single bin	0.067	0.025	0.011	0.000	0.897	1720	1728.4
Multi-ring			0.294	0.047	0.342	0.000	0.318	(1682)	(1624.2)
<i>Fully Contained (FC) Multi-GeV</i>									
Single-ring									
ν_e -like	4 e^\pm momentum	10 in $[-1, 1]$	0.621	0.090	0.100	0.033	0.156	705	671.3
$\bar{\nu}_e$ -like	4 e^\pm momentum	10 in $[-1, 1]$	0.546	0.372	0.009	0.010	0.063	2142	2193.7
μ -like	2 μ^\pm momentum	10 in $[-1, 1]$	0.003	0.001	0.992	0.002	0.002	2565	2573.8
Multi-ring									
ν_e -like	3 visible energy	10 in $[-1, 1]$	0.557	0.102	0.117	0.040	0.184	907	915.5
$\bar{\nu}_e$ -like	3 visible energy	10 in $[-1, 1]$	0.531	0.270	0.041	0.022	0.136	745	773.8
μ -like	4 visible energy	10 in $[-1, 1]$	0.027	0.004	0.913	0.005	0.051	2310	2294.0
Other	4 visible energy	10 in $[-1, 1]$	0.275	0.029	0.348	0.049	0.299	1808	1772.6

(low energies needed for δ_{CP})

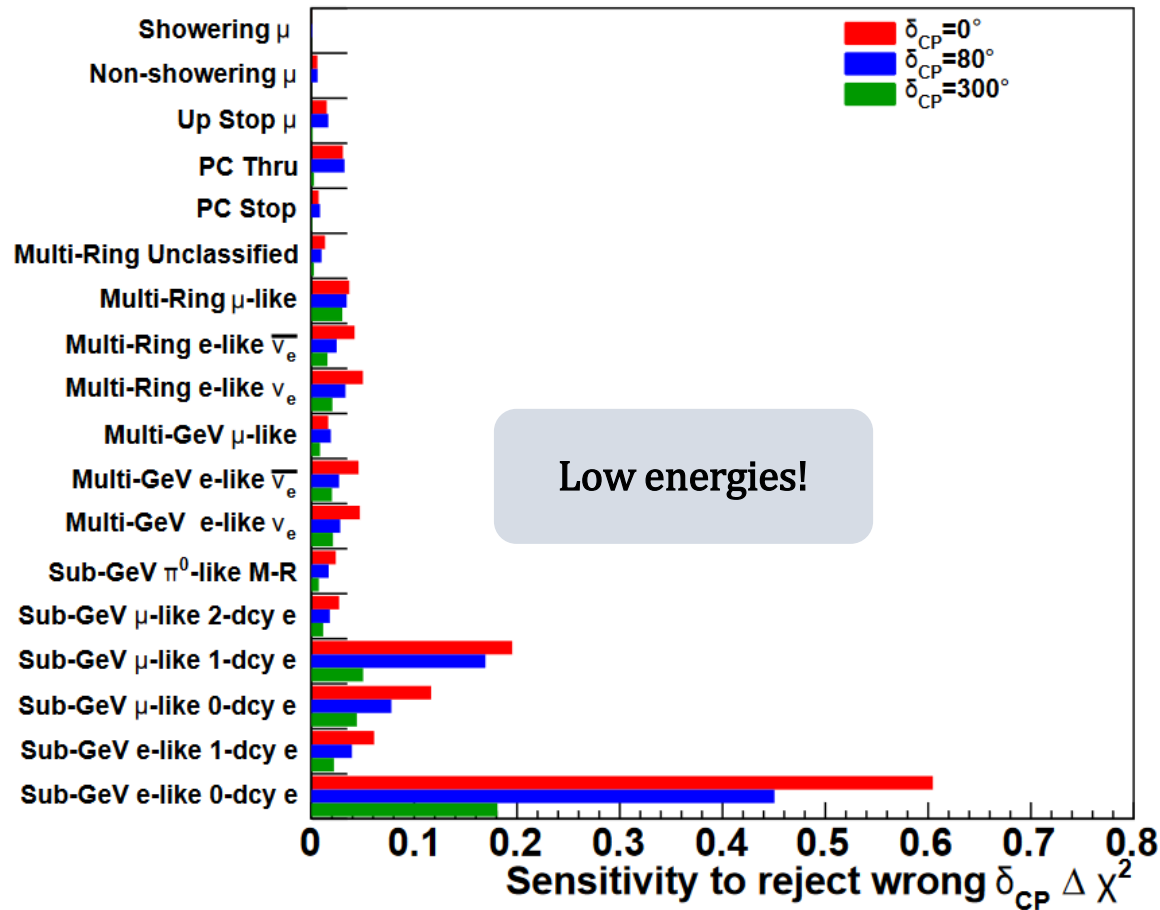
(high energies needed for MH)

(example from SK analysis)

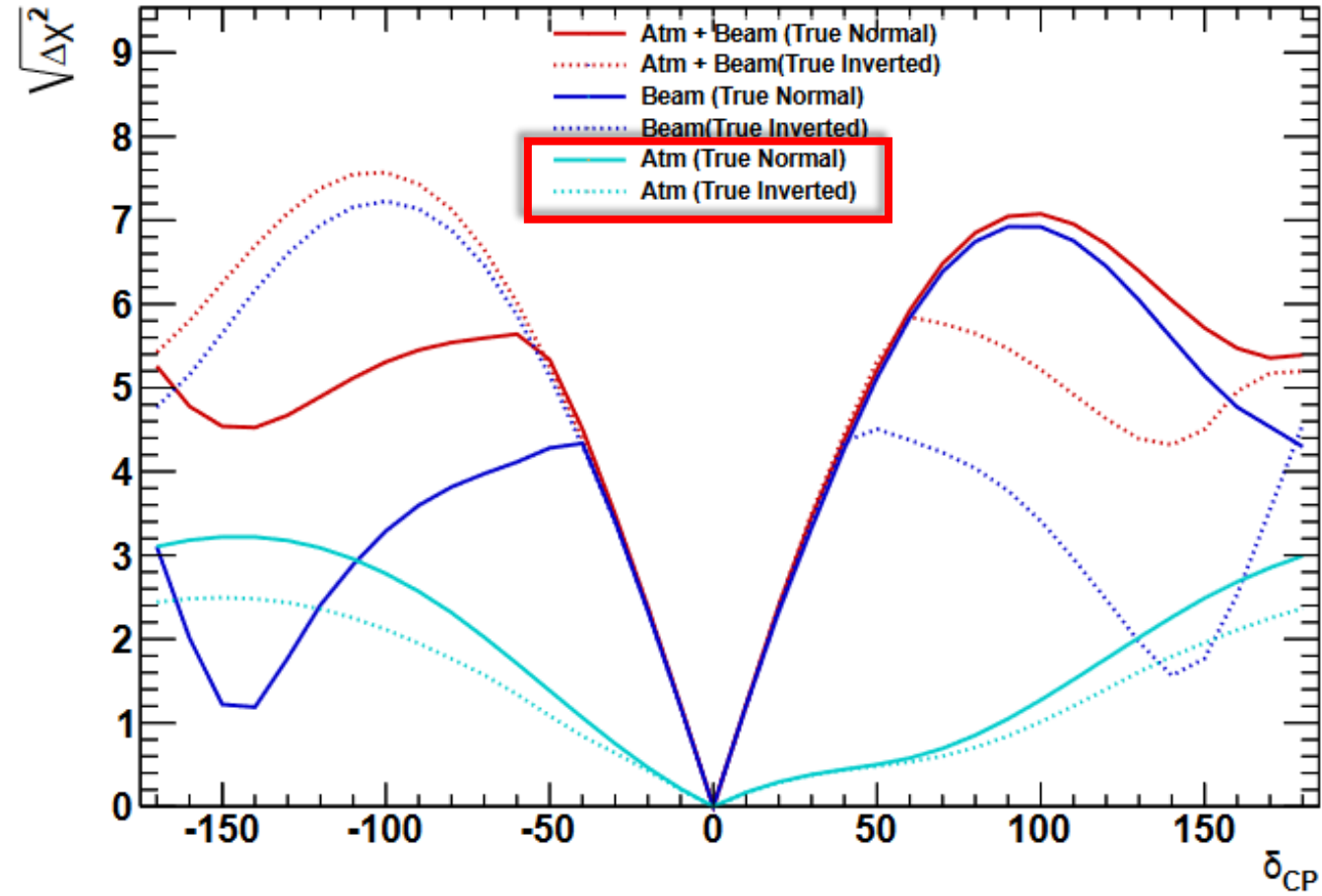
Phys. Rev. D 97, 072001 (2018)

Sub-GeV, 0-decay e-like events drive δ_{CP} sensitivity.

(We want sub-GeV ν_e !)



(10 yrs Hyper-K)

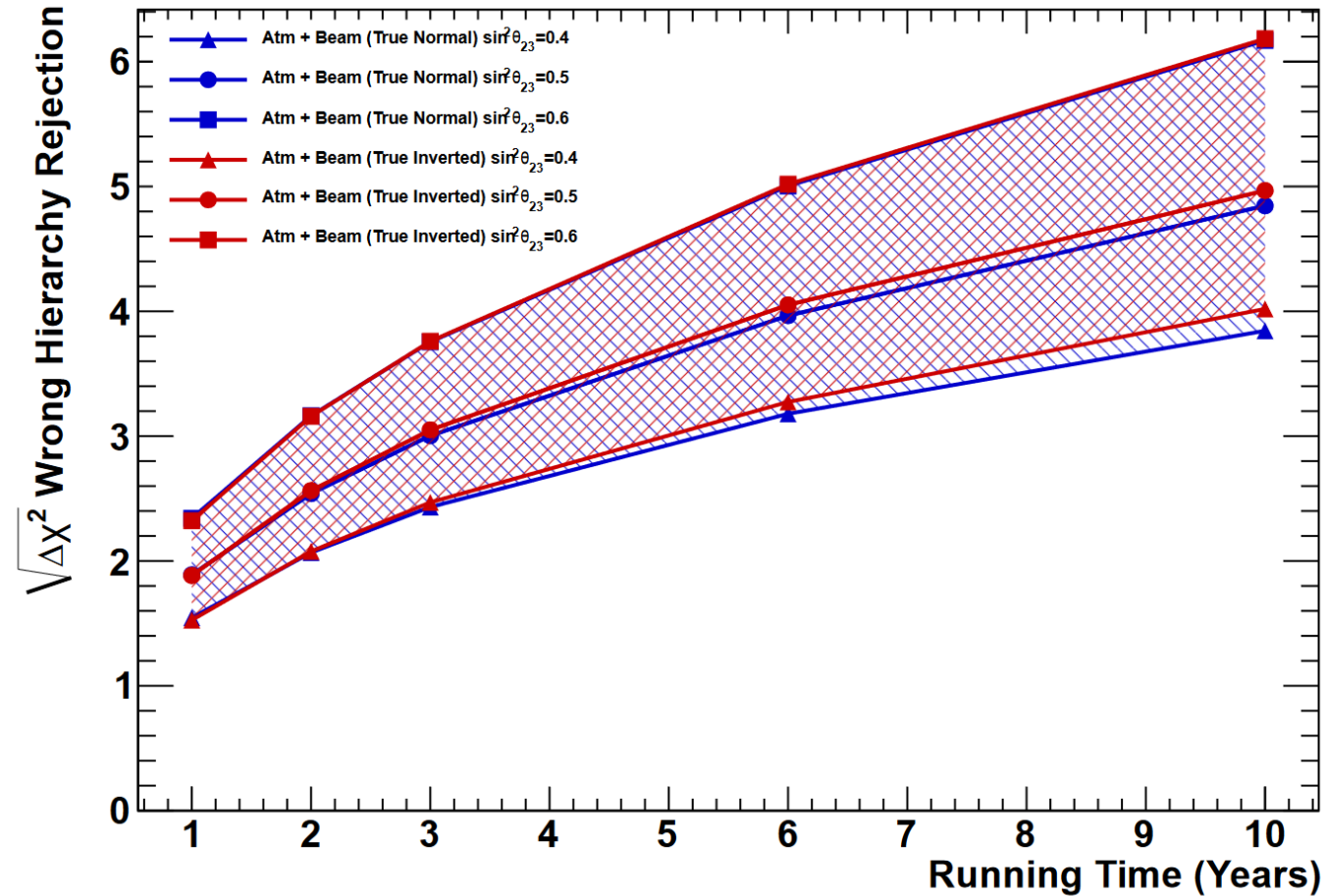
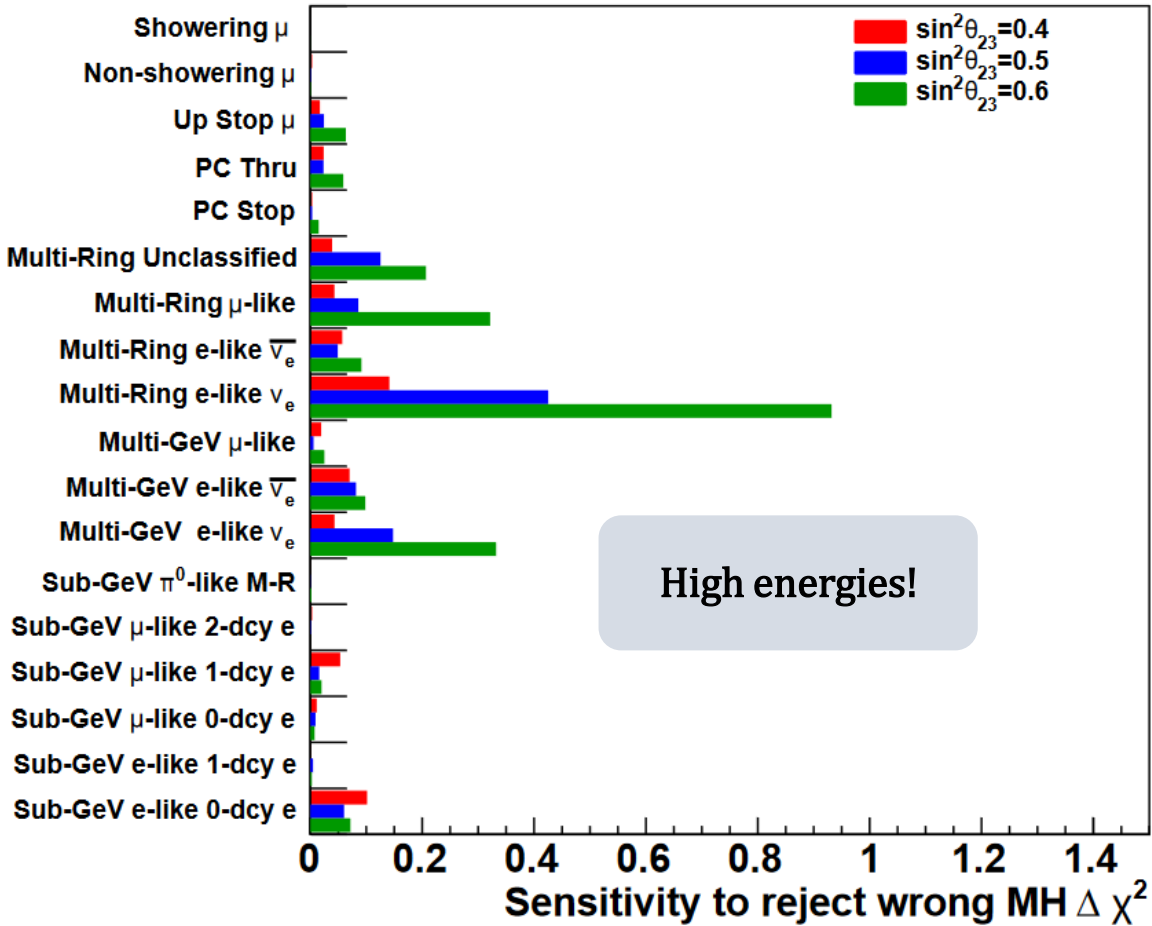


M. Jiang (2019), PhD Thesis, Kyoto University

Hyper-K Design Report (2018)

Multi-ring ν_e events drive the MH sensitivity.

(We want multi-GeV ν_e !)

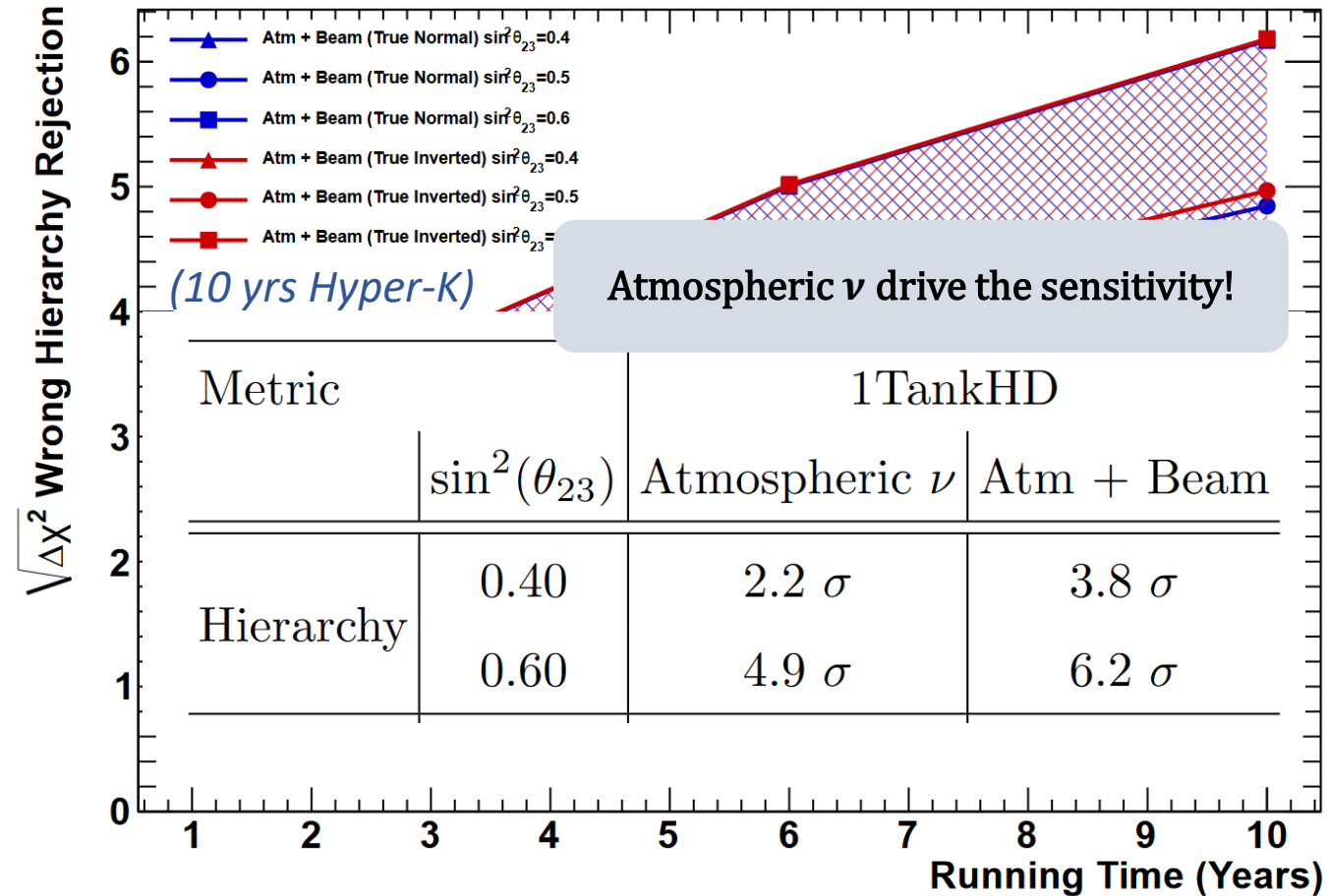
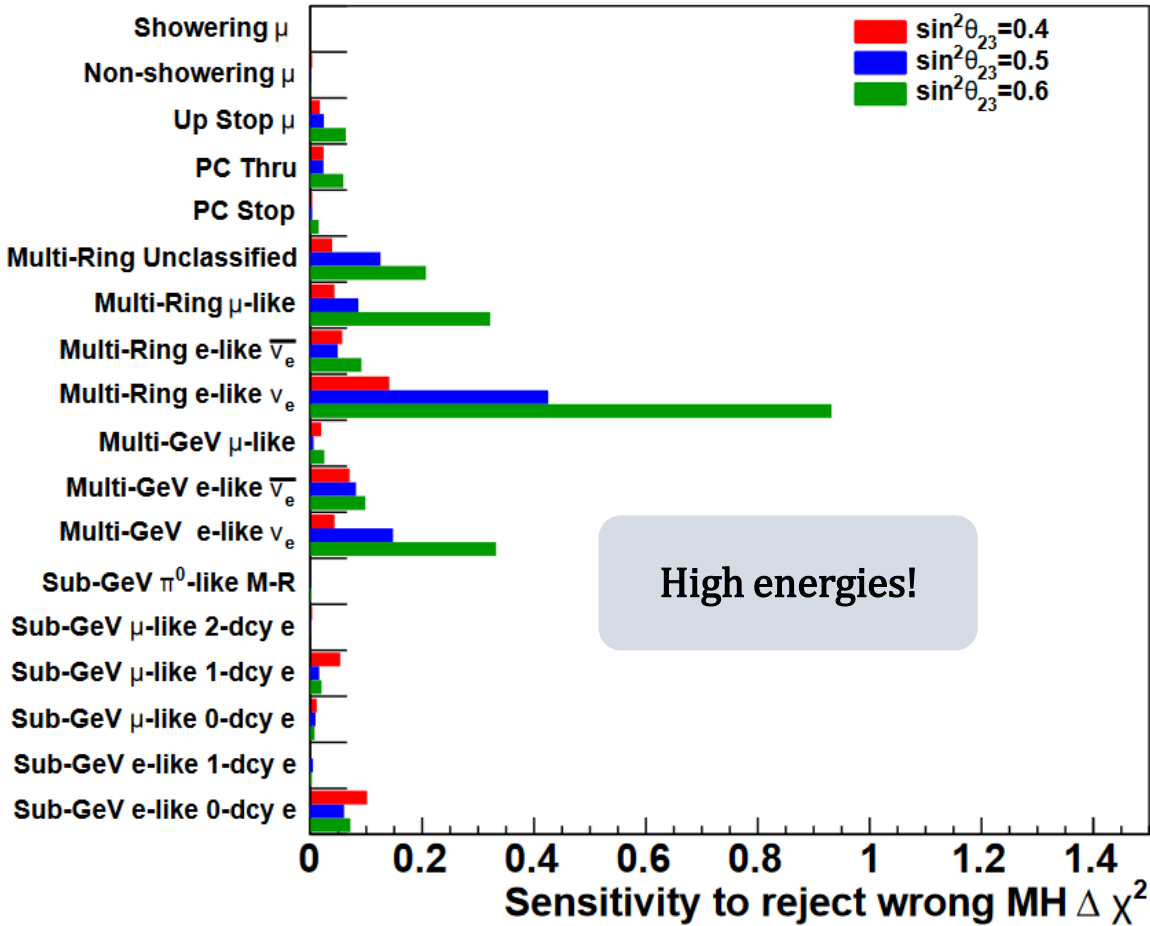


M. Jiang (2019), PhD Thesis, Kyoto University

Hyper-K Design Report (2018)

Multi-ring ν_e events drive the MH sensitivity (more than beam)!

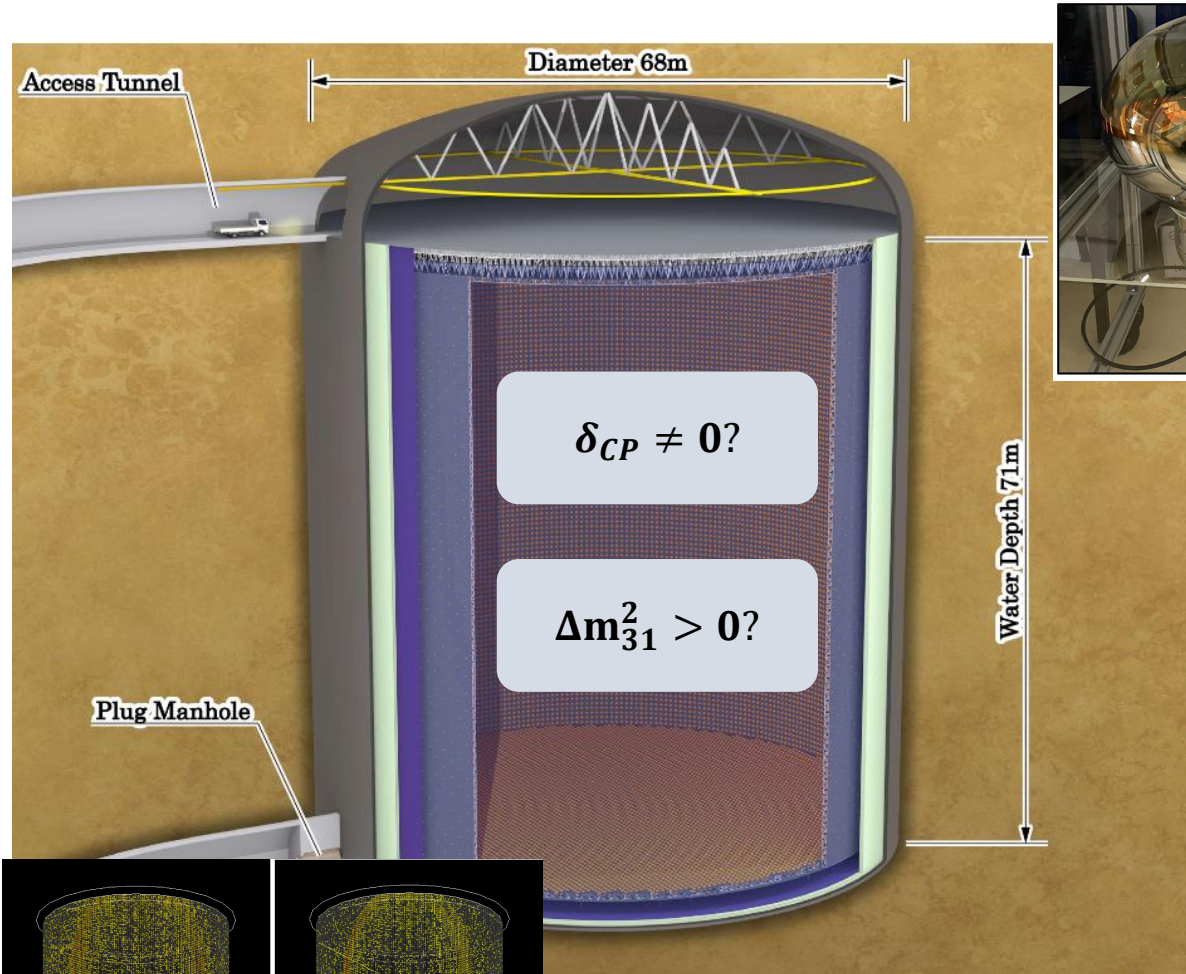
(We want multi-GeV ν_e !)



M. Jiang (2019), PhD Thesis, Kyoto University

Hyper-K Design Report (2018)

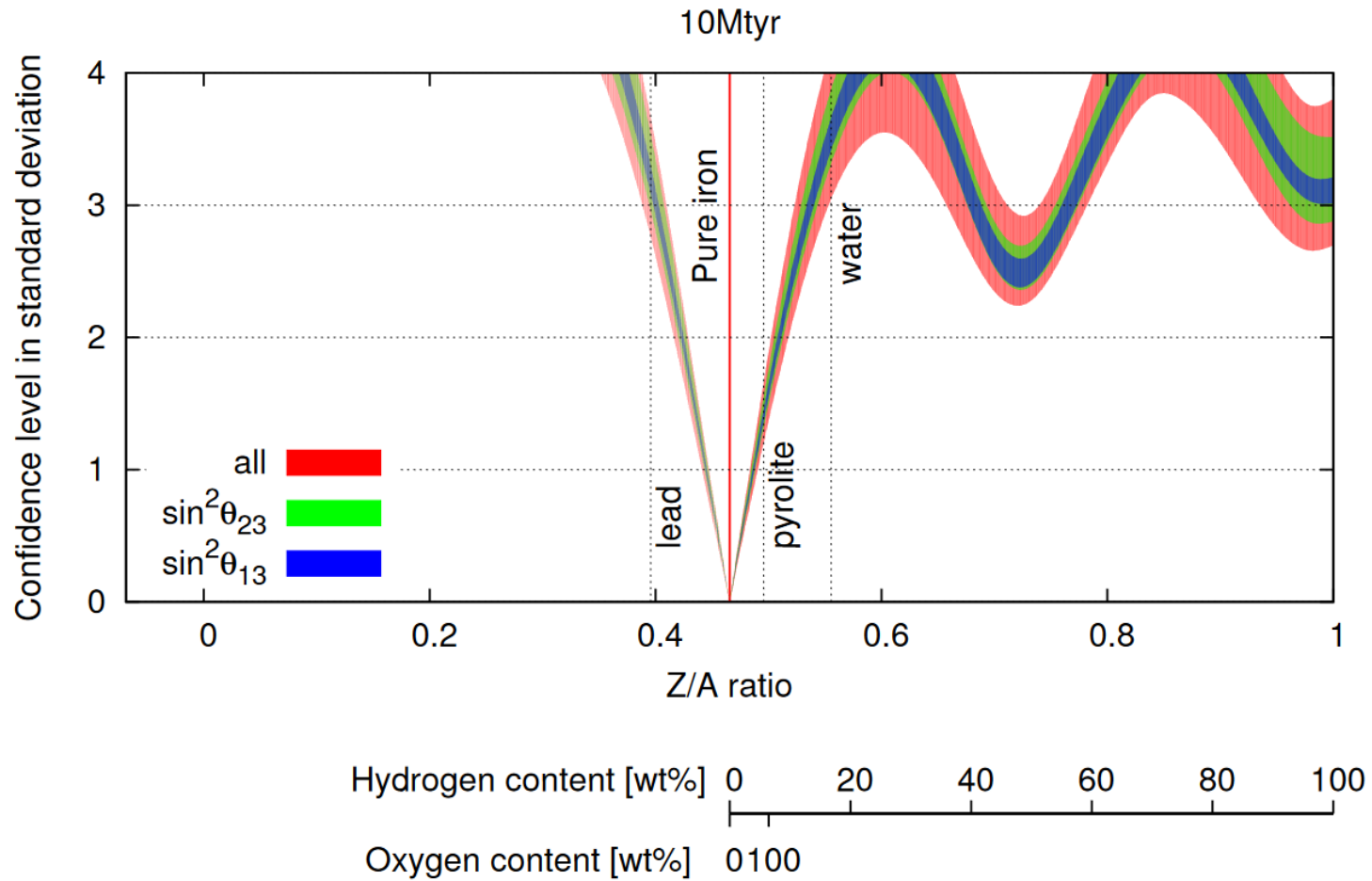
Summary of atmospheric neutrinos at Hyper-Kamiokande



- **Atmospheric neutrinos** are created by interactions of primary cosmic rays in the atmosphere.
- **Energies** span $\mathcal{O}(100 \text{ MeV})$ to as high as $\mathcal{O}(10000 \text{ GeV})$ with **baselines** between $\mathcal{O}(10 \text{ km})$ to $\mathcal{O}(10000 \text{ km})$.
- **Matter effects** on neutrino oscillations permit atmospheric neutrinos to **probe CP-violation** and neutrino **mass hierarchy**.
- **Hyper-Kamiokande** is a next-generation water Cherenkov experiment with **fiducial volume $\sim 8X$** that of Super-Kamiokande to **start taking data in 2027**.
- The **reconstruction and PID capabilities of Hyper-K** will lead to studying **data samples enhanced with ν_e** at sub-GeV and multi-GeV energies.
- Atmospheric **sub-GeV ν_e** samples at Hyper-K will be **sensitive to δ_{CP}** .
- Atmospheric **multi-GeV ν_e** will provide more sensitivity to the neutrino **mass hierarchy** compared to beam ν .
- **Mass hierarchy** determination **assists δ_{CP}** sensitivity.

Backup

Hyper-K will be sensitive to Earth composition.



Hyper-K Design Report (2018)

Neutrino oscillations in the 2-flavor picture

$$|\nu_\alpha\rangle = \sum_i U_{\alpha i} |\nu_i\rangle$$

$$|\nu_e\rangle = \cos\theta |\nu_1\rangle + \sin\theta |\nu_2\rangle$$

$$|\nu_e(t, \vec{x})\rangle = e^{-ip_1x} \cos\theta |\nu_1\rangle + e^{-ip_2x} \sin\theta |\nu_2\rangle$$

$$p_i x = E_i t - \vec{p}_i \cdot \vec{x} \approx (E_i - p_i)L, \quad x = L \approx t$$

$$p_i x \approx (E - p_i)L, \quad E_i \approx E, \forall i$$

$$p_i x \approx \frac{m_i^2 L}{2E}, \quad p_i \approx E \Rightarrow \sqrt{E^2 - m_i^2} = E \sqrt{1 - \frac{m_i^2}{E^2}} \approx E - \frac{m_i^2}{2E}$$

(approximations)

$$|\nu_e(L)\rangle = e^{-\frac{im_1^2 L}{2E}} \cos\theta |\nu_1\rangle + e^{-\frac{im_2^2 L}{2E}} \sin\theta |\nu_2\rangle$$

$$P_{ee} = |\langle \nu_e | \nu_e(L) \rangle|^2 = 1 - \sin^2 2\theta \sin^2 \left(\frac{\Delta m^2 L}{4E} \right)$$

MSW effect and its influence on supernova neutrinos

A new matter basis...

$$H_V = \frac{\Delta m^2}{4E} \begin{pmatrix} -\cos 2\theta & \sin 2\theta \\ \sin 2\theta & \cos 2\theta \end{pmatrix} + \sqrt{2}G_F n_e \begin{pmatrix} 1 & 0 \\ 0 & 0 \end{pmatrix}$$

Resonance occurs for $H_{ee} = H_{xx}$...

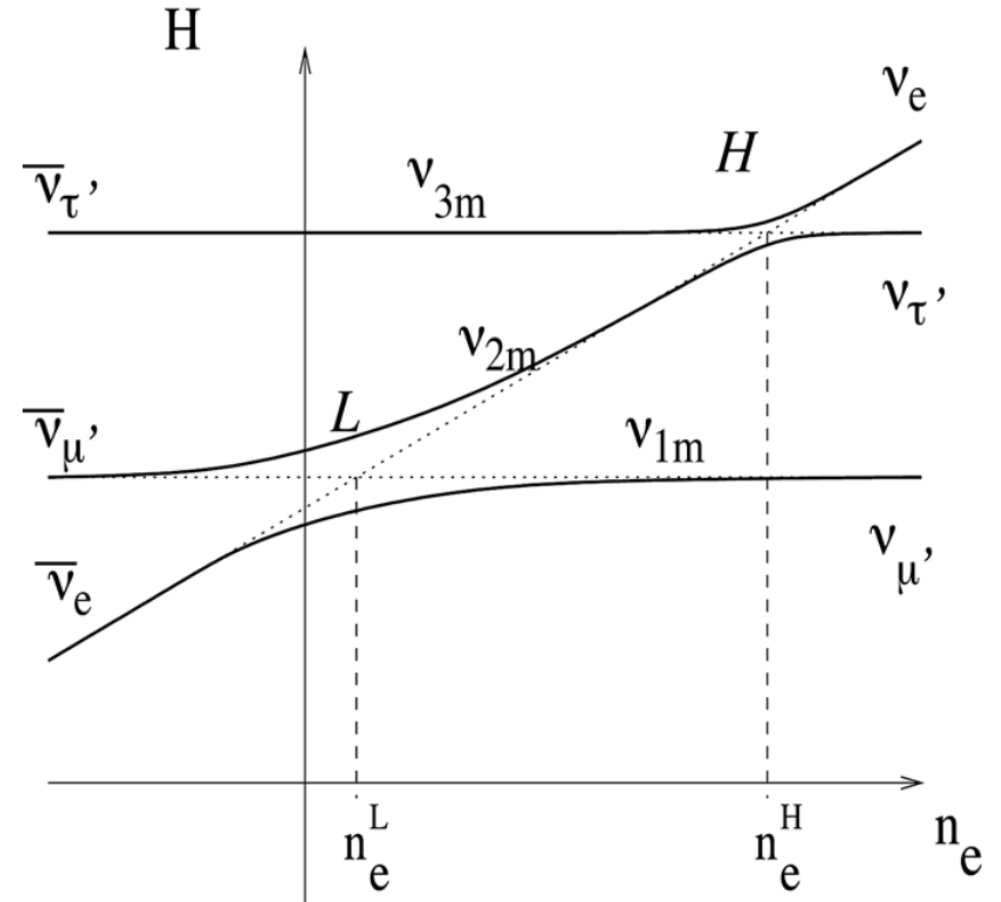
$$\tan \theta_M = \frac{2H_{ex}}{H_{ee} - H_{xx}} = \frac{\frac{\Delta m^2}{2E} \sin 2\theta}{-\frac{\Delta m^2}{4E} \cos 2\theta + \sqrt{2}G_F n_e}$$

$$-\cos 2\theta \frac{\Delta m^2}{4E} + \sqrt{2}G_F n_e = \cos 2\theta \frac{\Delta m^2}{4E}$$

$$\sqrt{2}G_F n_e = \cos 2\theta \frac{\Delta m^2}{2E}$$

(1) $\Delta m_{21}^2 > 0$ from Sun

(2) $\text{sign}(\Delta m_{31}^2)$ unknown



Source: C. Volpe (2013), *Ann. Phys.* **525**, 8-9, p. 588

MSW effect and its influence on supernova neutrinos

(NH, ν_e)

$$F_{\nu_e, NH} = [P_H(1 - P_L) \sin^2 \theta_{12} + P_H P_L \cos^2 \theta_{12} + (1 - P_H) \sin^2 \theta_{13}] F_{\nu_e}^0 + \dots$$

$$F_{\nu_e, NH} = [P_H(1 - P_L) \sin^2 \theta_{12} + P_H P_L \cos^2 \theta_{12} + 0] F_{\nu_e}^0 + \dots, \quad \sin^2 \theta_{13} \approx 0$$

$$F_{\nu_e, NH} = [P_H \sin^2 \theta_{12} + 0 + 0] F_{\nu_e}^0 + \dots, \quad P_L = 0$$

$$F_{\nu_e, NH} = [0 + 0 + 0] F_{\nu_e}^0 + \dots, \quad P_H = 0$$

$$F_{\nu_e, NH} = p F_{\nu_e}^0 + (1 - p) F_{\nu_x}^0, \quad p = 0$$

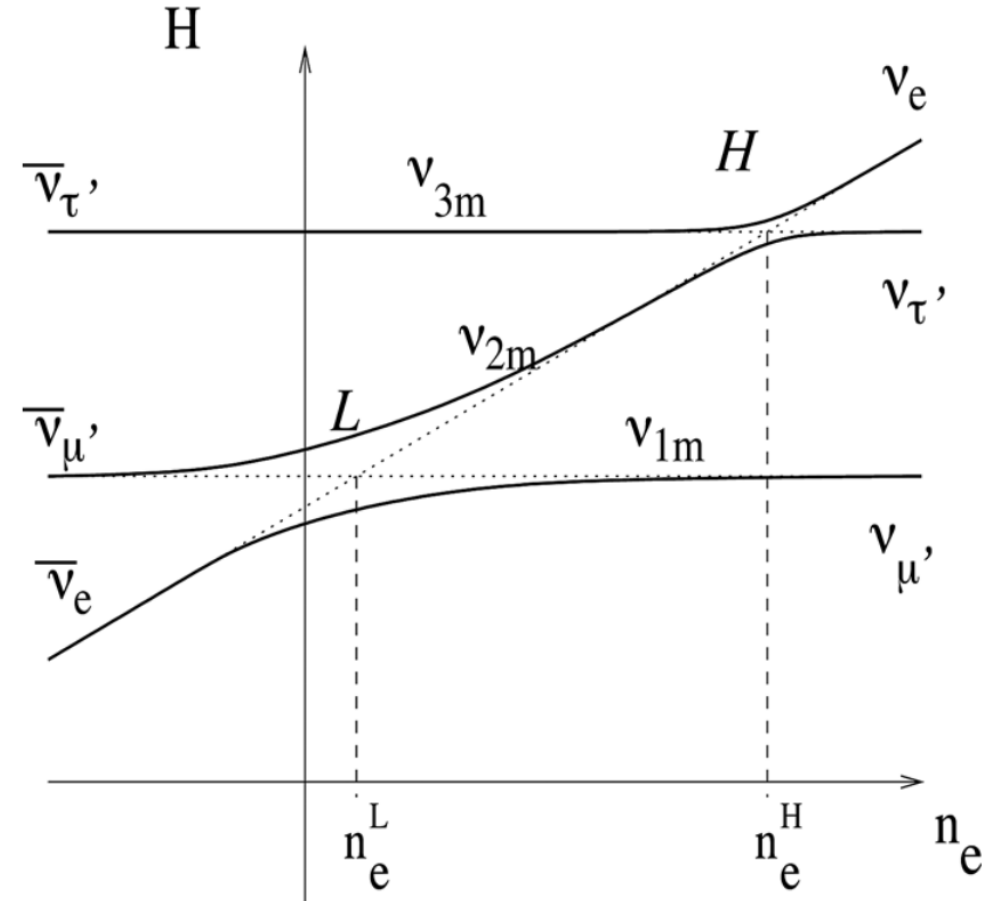
(NH, $\bar{\nu}_e$)

$$F_{\bar{\nu}_e, NH} = \cos^2 \theta_{12} F_{\bar{\nu}_e}^0 + \sin^2 \theta_{12} F_{\nu_{\mu'}}^0 + \sin^2 \theta_{13} F_{\nu_{\tau'}}^0$$

$$F_{\bar{\nu}_e, NH} = \cos^2 \theta_{12} F_{\bar{\nu}_e}^0 + \sin^2 \theta_{12} F_{\nu_{\mu'}}^0, \quad \sin^2 \theta_{13} \approx 0$$

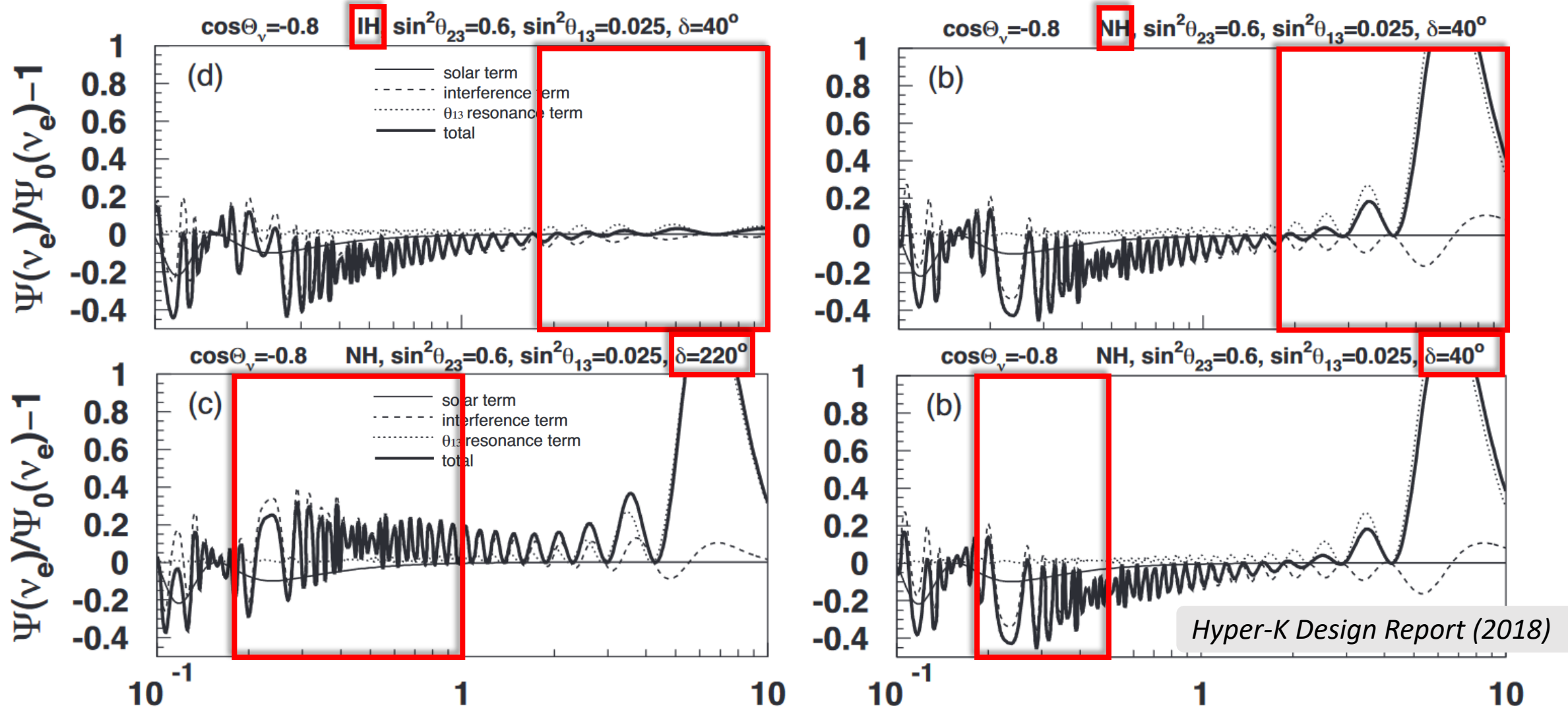
$$F_{\bar{\nu}_e, NH} = \cos^2 \theta_{12} F_{\bar{\nu}_e}^0 + (1 - \cos^2 \theta_{12}) F_{\nu_x}^0, \quad F_{\nu_{\mu'}}^0 = F_{\nu_x}^0$$

$$F_{\bar{\nu}_e, NH} = \bar{p} F_{\bar{\nu}_e}^0 + (1 - \bar{p}) F_{\nu_x}^0, \quad \bar{p} = \cos^2 \theta_{12} \approx 0.68$$

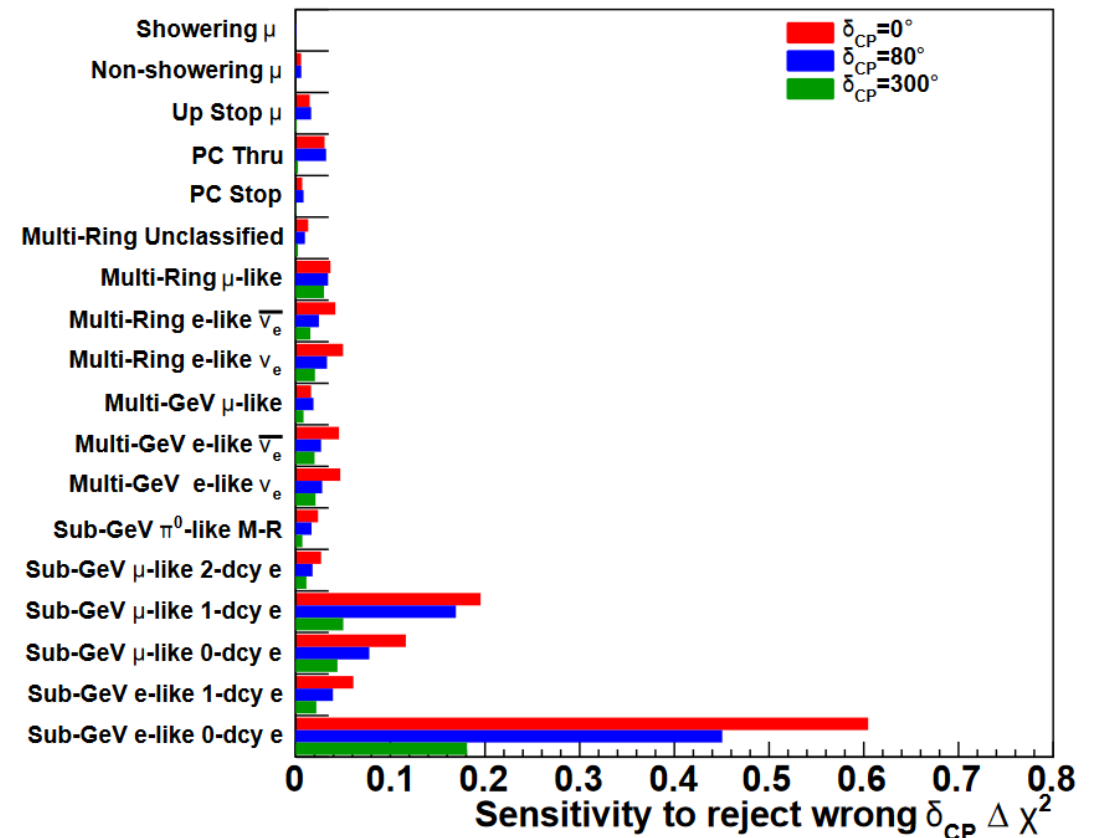
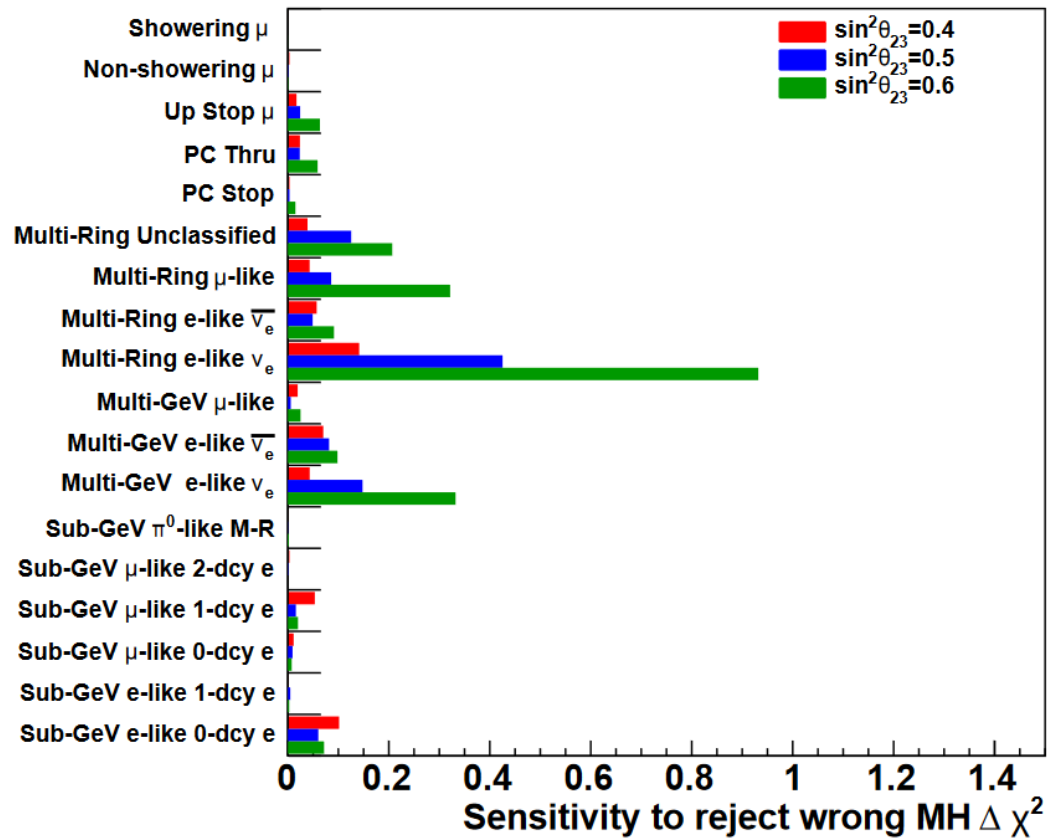


Source: C. Volpe (2013), *Ann. Phys.* **525**, 8-9, p. 588

We want to study sub-GeV and multi-GeV atmospheric ν_e !

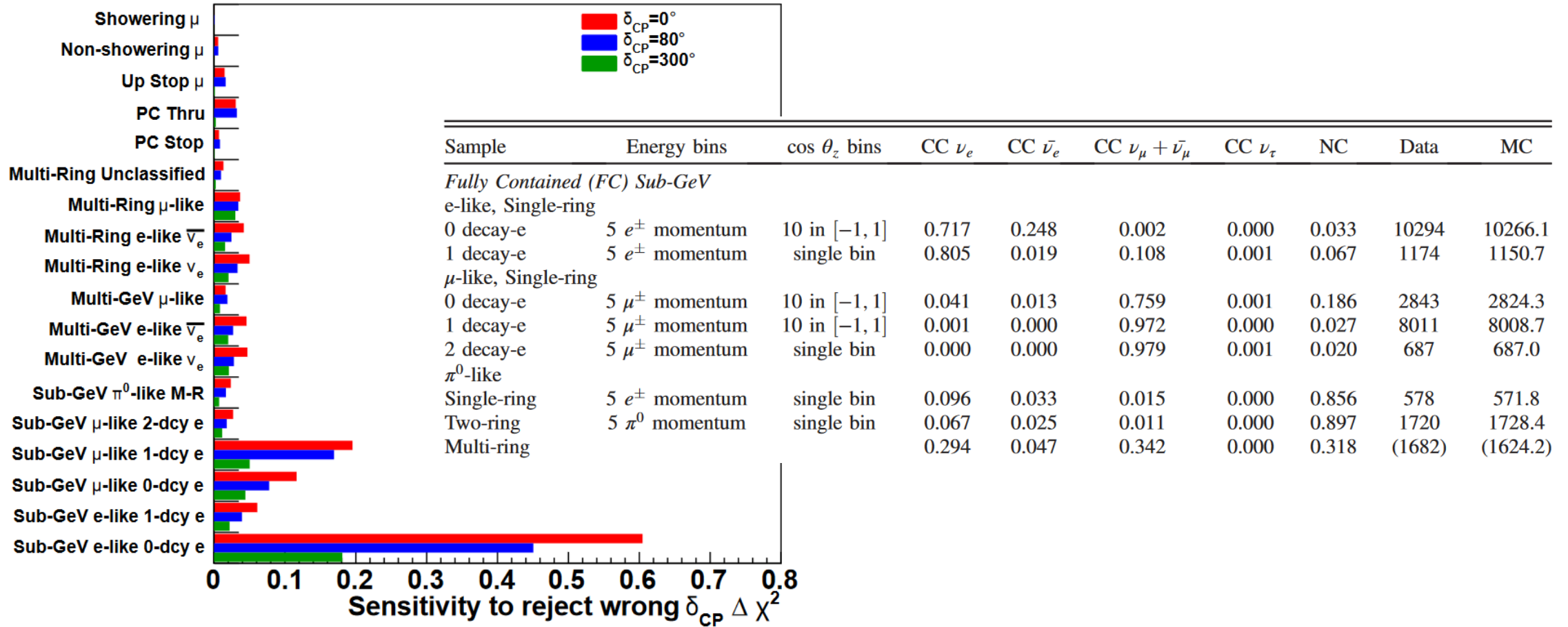


SK sensitivities compared for δ_{CP} and MH rejection



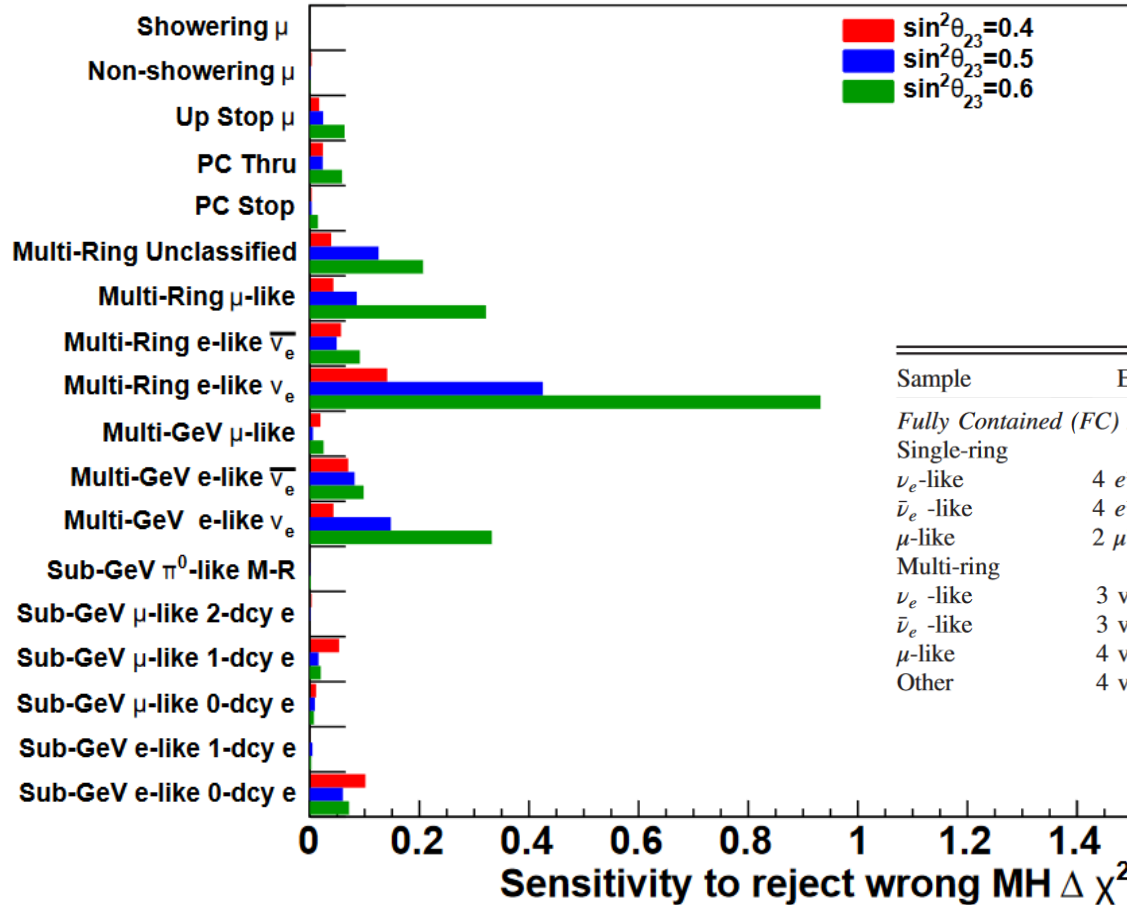
M. Jiang (2019), PhD Thesis, Kyoto University

HK δ_{CP} rejection sensitivity with main sample



M. Jiang (2019), PhD Thesis, Kyoto University

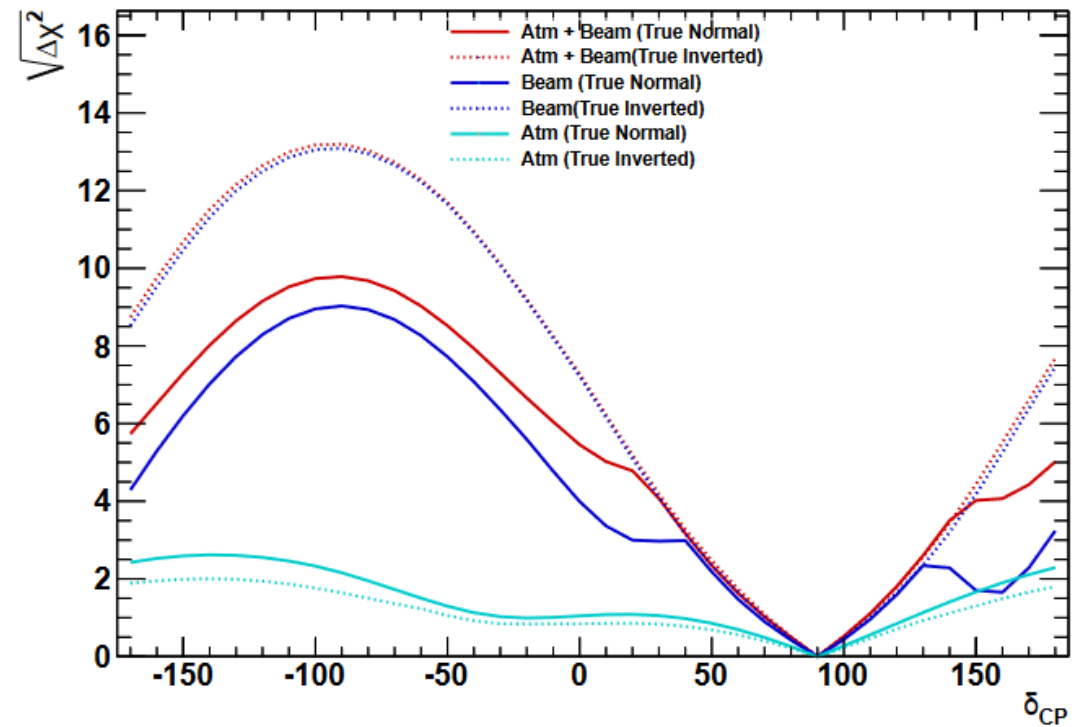
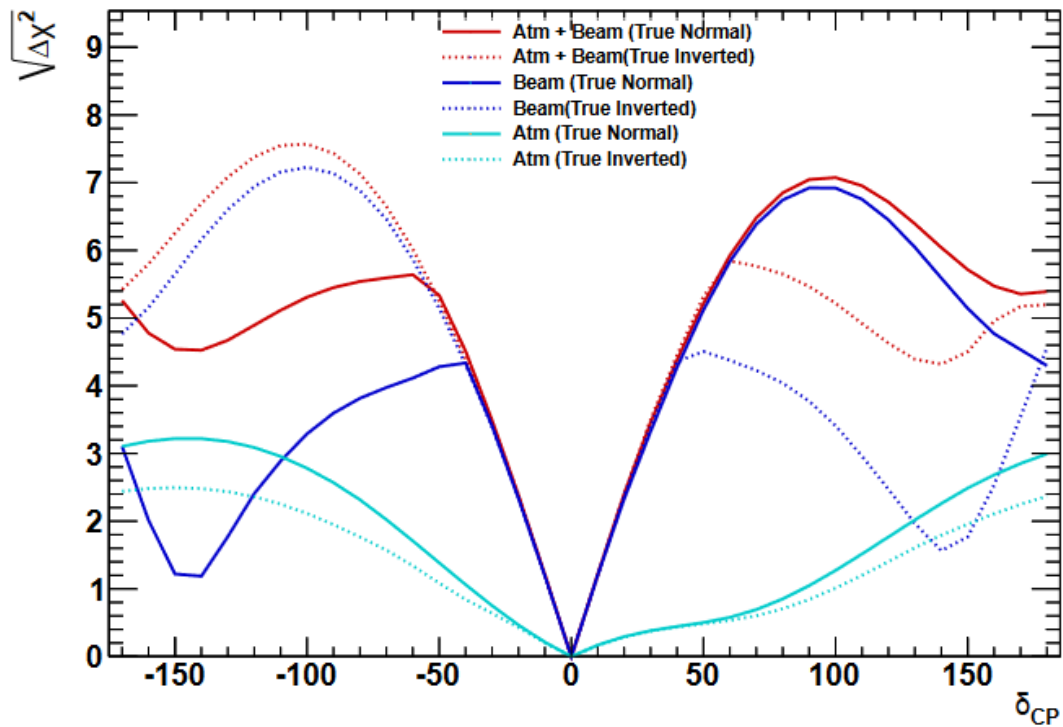
HK MH rejection sensitivity with main sample



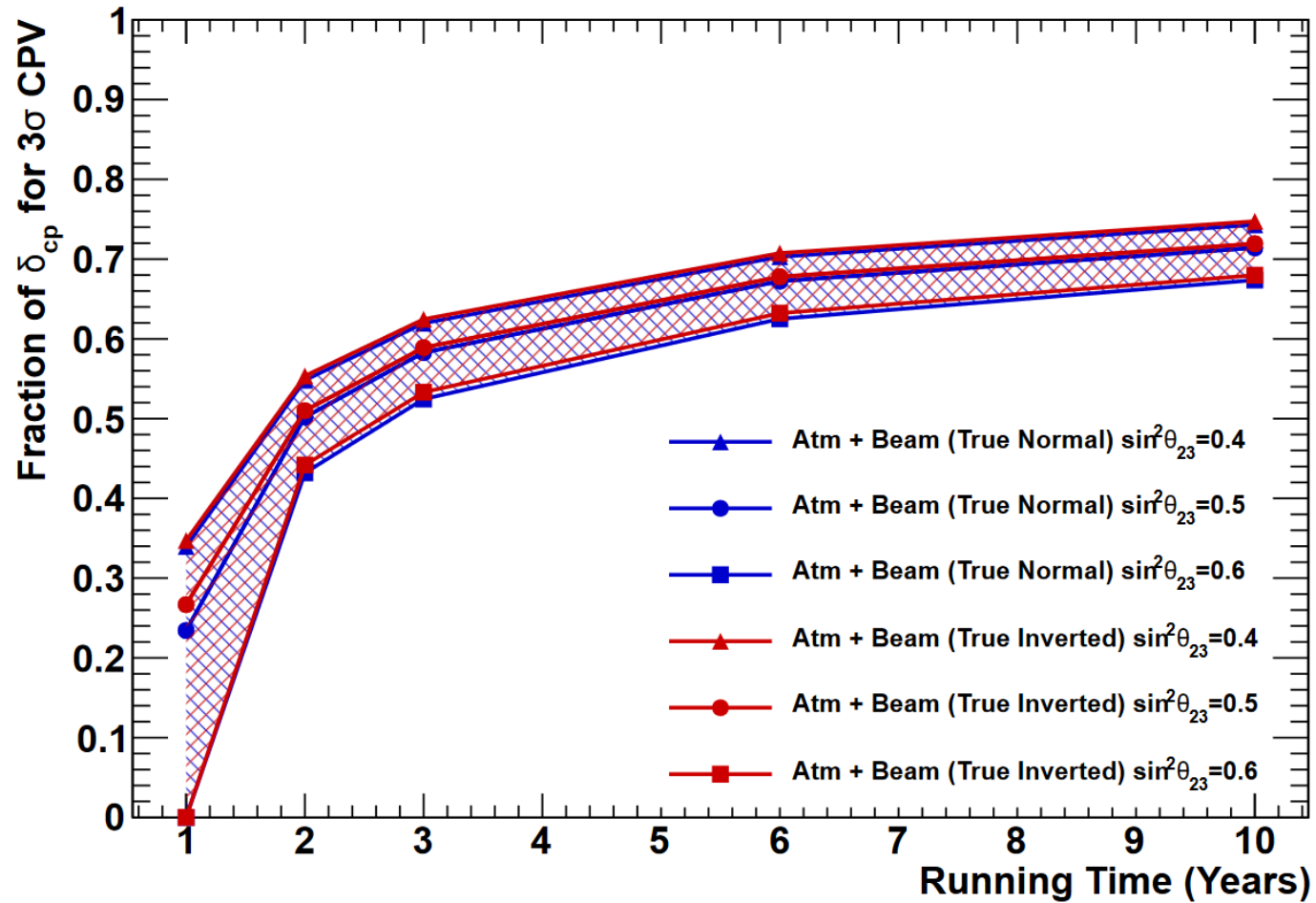
Sample	Energy bins	$\cos\theta_z$ bins	CC ν_e	CC $\bar{\nu}_e$	CC $\nu_\mu + \bar{\nu}_\mu$	CC ν_τ	NC	Data	MC
<i>Fully Contained (FC) Multi-GeV</i>									
Single-ring									
ν_e -like	4 e^\pm momentum	10 in $[-1, 1]$	0.621	0.090	0.100	0.033	0.156	705	671.3
$\bar{\nu}_e$ -like	4 e^\pm momentum	10 in $[-1, 1]$	0.546	0.372	0.009	0.010	0.063	2142	2193.7
μ -like	2 μ^\pm momentum	10 in $[-1, 1]$	0.003	0.001	0.992	0.002	0.002	2565	2573.8
Multi-ring									
ν_e -like	3 visible energy	10 in $[-1, 1]$	0.557	0.102	0.117	0.040	0.184	907	915.5
$\bar{\nu}_e$ -like	3 visible energy	10 in $[-1, 1]$	0.531	0.270	0.041	0.022	0.136	745	773.8
μ -like	4 visible energy	10 in $[-1, 1]$	0.027	0.004	0.913	0.005	0.051	2310	2294.0
Other	4 visible energy	10 in $[-1, 1]$	0.275	0.029	0.348	0.049	0.299	1808	1772.6

M. Jiang (2019), PhD Thesis, Kyoto University

HK δ_{CP} rejection for both $\delta_{CP} = 0^\circ, 90^\circ$

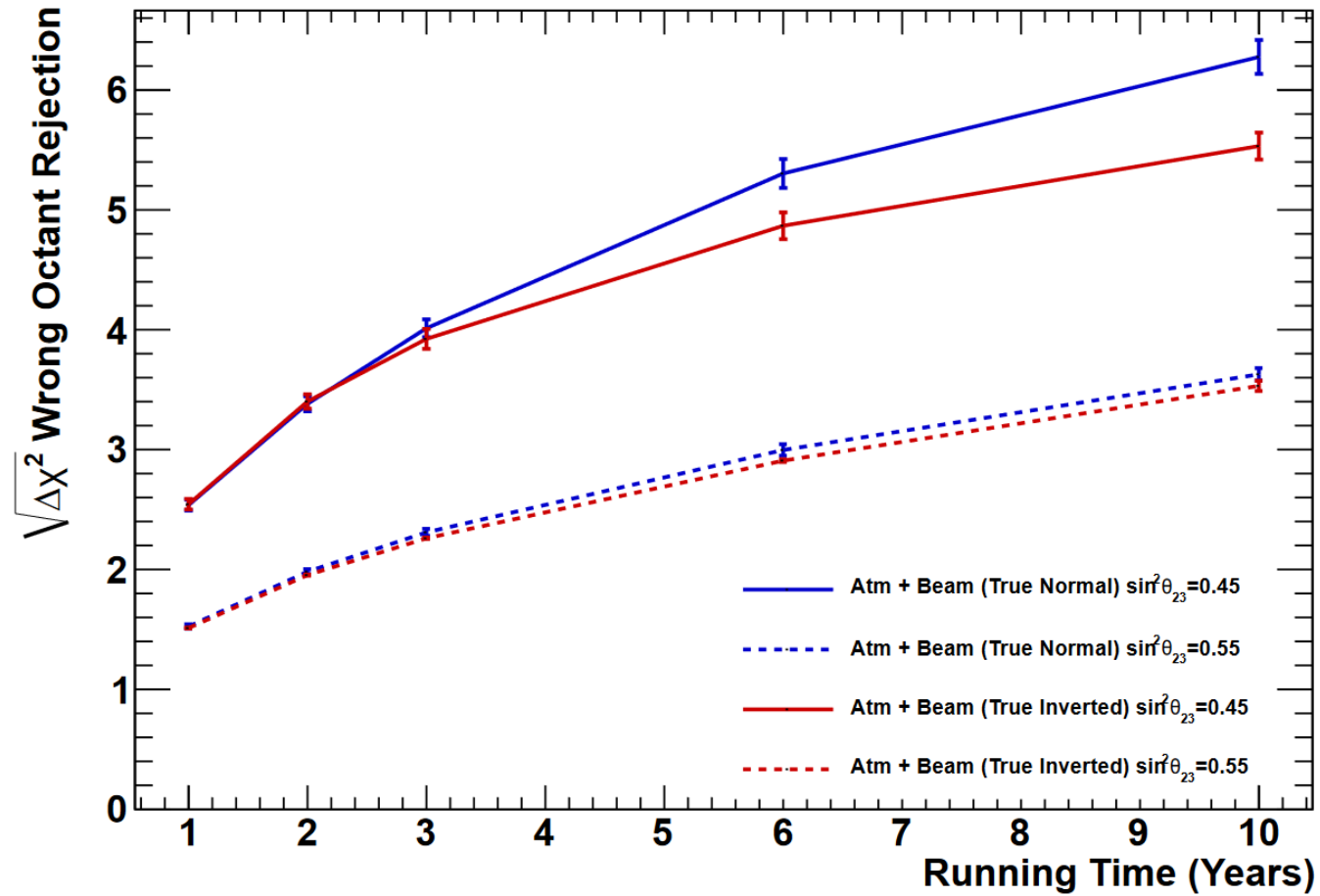


HK fraction of δ_{CP} values covered at 3σ



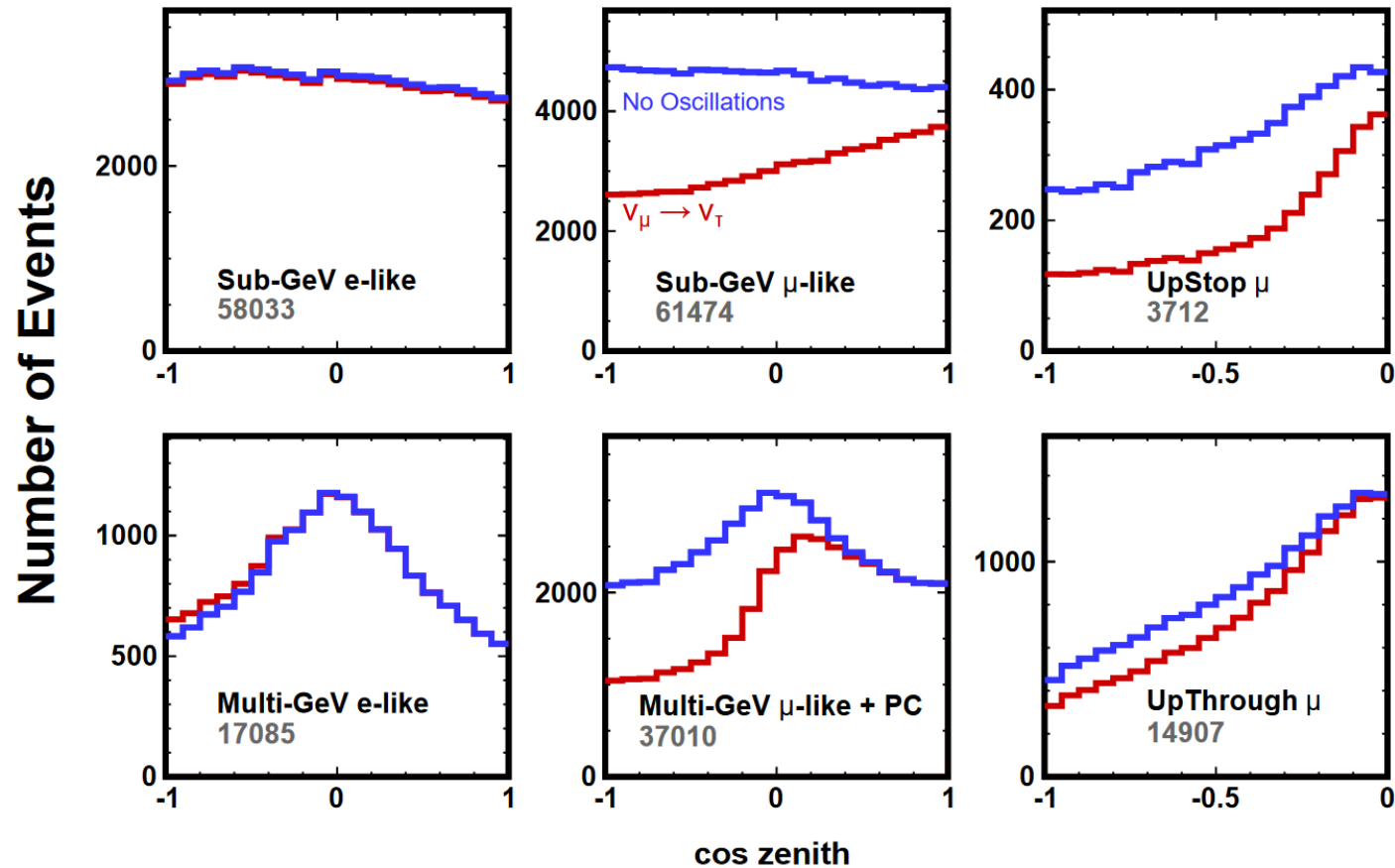
Hyper-K Design Report (2018)

HK wrong octant rejection



Hyper-K Design Report (2018)

Atmospheric samples in HK with and w/o oscillations



Hyper-K Design Report (2018)

Vertex reconstruction SK/HK

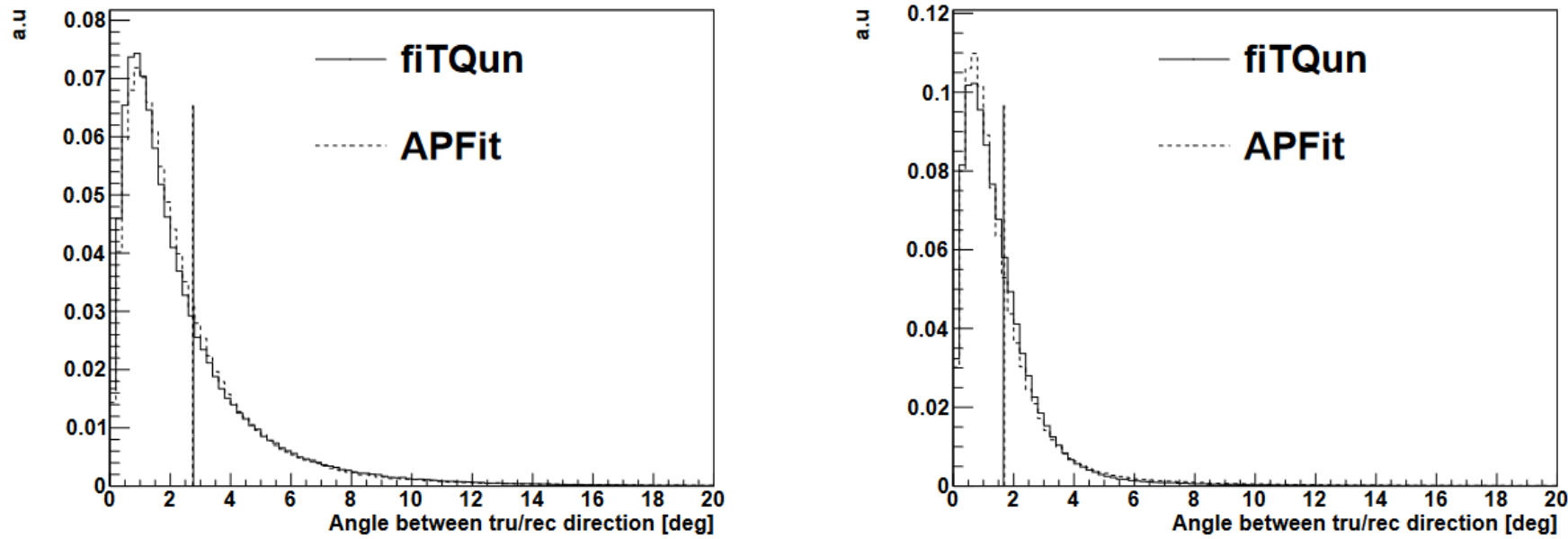


FIGURE 6.6: Single-ring electron (left) and muon (right) direction resolution for FC CCQE events in atmospheric neutrino MC, compared between APFit (dashed line) and fiTQun (solid line). The resolution is defined as the 68 percentile of the respective distributions which is shown by corresponding vertical line.

Vertex reconstruction SK/HK

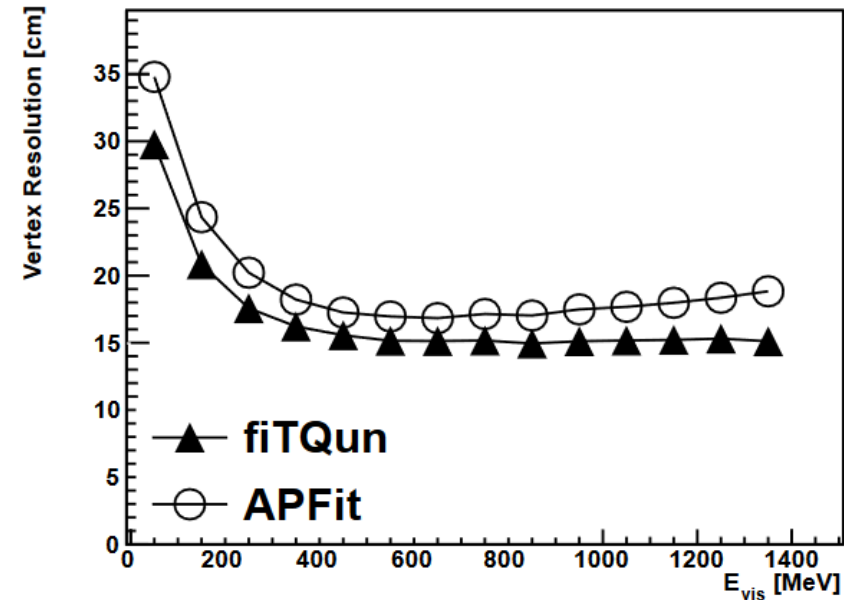
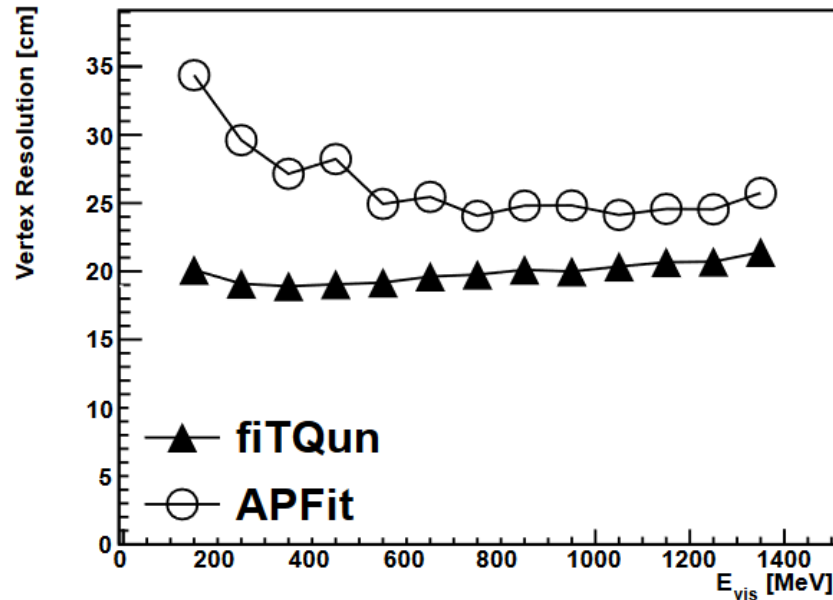


FIGURE 6.5: Vertex resolution of FC single-ring charged current quasi-elastic (CCQE) event as a function of visible energy. Left figure is for CC ν_e events and right figure is for CC ν_μ events. The performance of fiTQun is indicated by the full triangles, while that for APFit is indicated by the open circles.

Direction reconstruction SK/HK

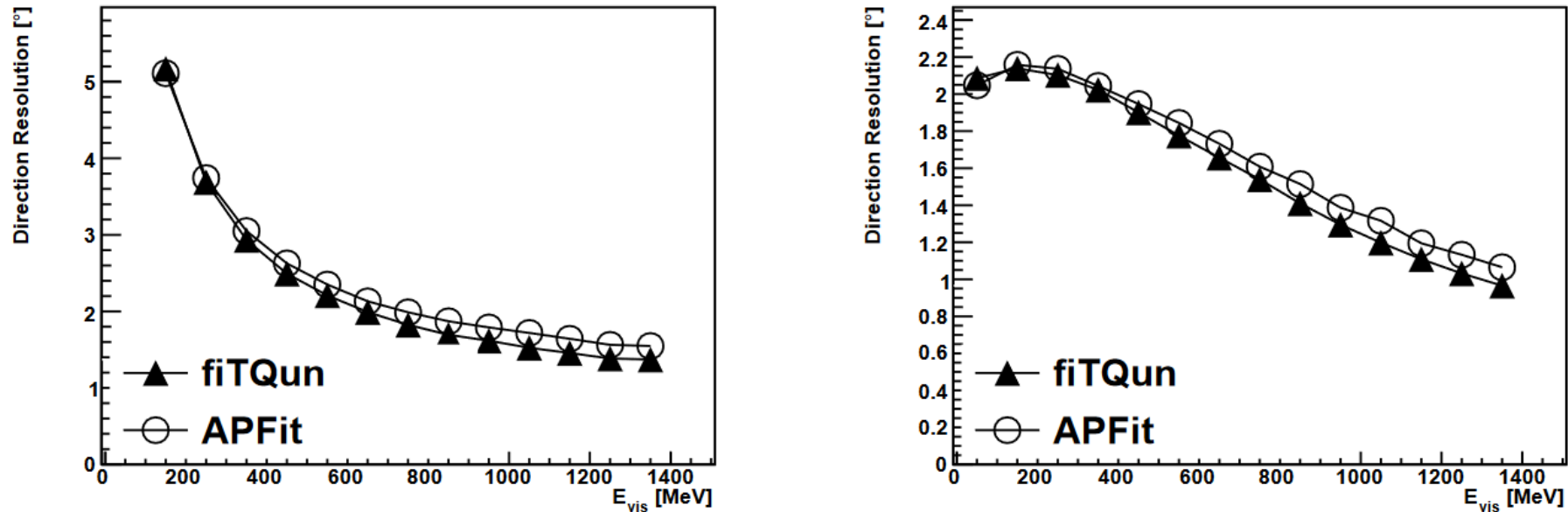


FIGURE 6.7: Direction resolution of single-ring electron (left) and muon (right) events in the FC CCQE event sample in the atmospheric neutrino MC, plotted as a function of visible energy. The full triangles indicate the performance of fiTQun and the open circles are for APFit.

Direction reconstruction SK/HK

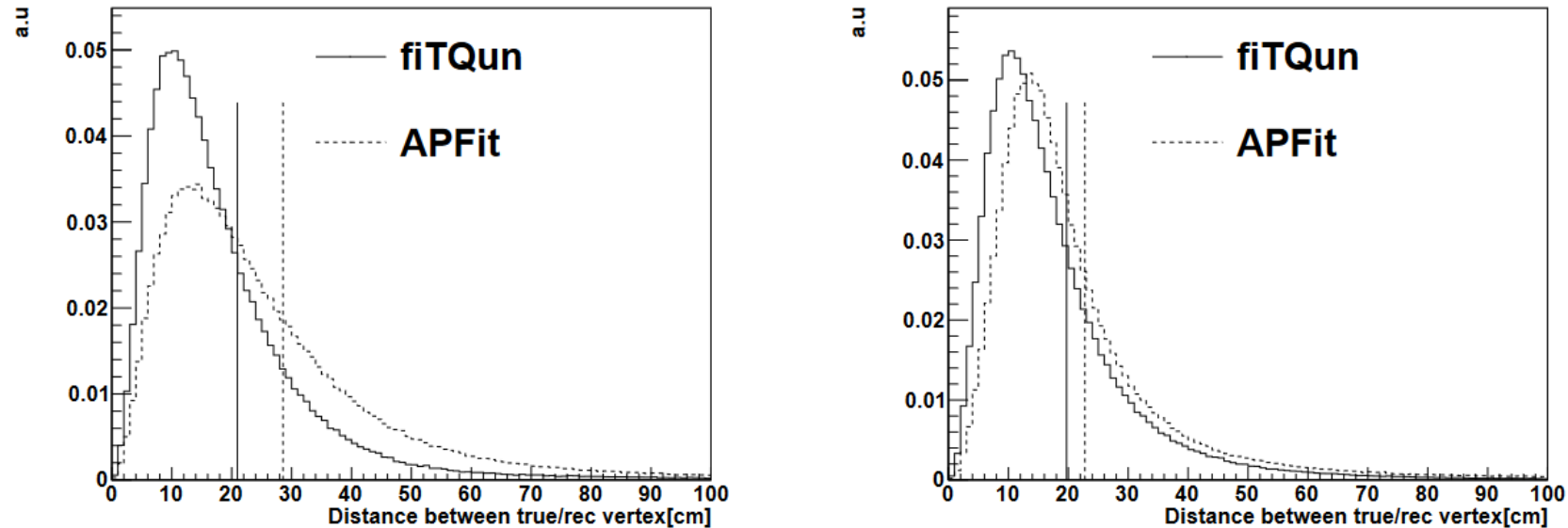


FIGURE 6.4: Single-ring electron(left) and muon(right) vertex resolution for FC true-fiducial CCQE events in atmospheric neutrino MC, compared between APFit(dashed line) and fiTQun(solid line). The resolution is defined as the 68 percentile of the respective distributions, which is shown by corresponding vertical line.

Energy reconstruction SK/HK

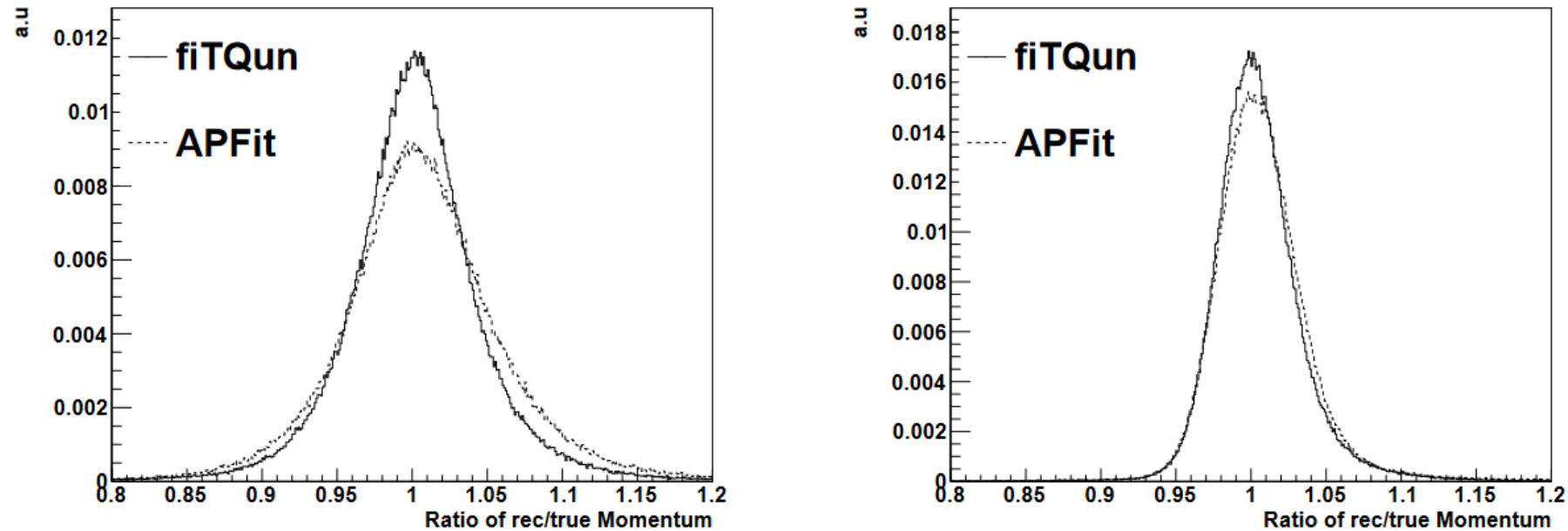
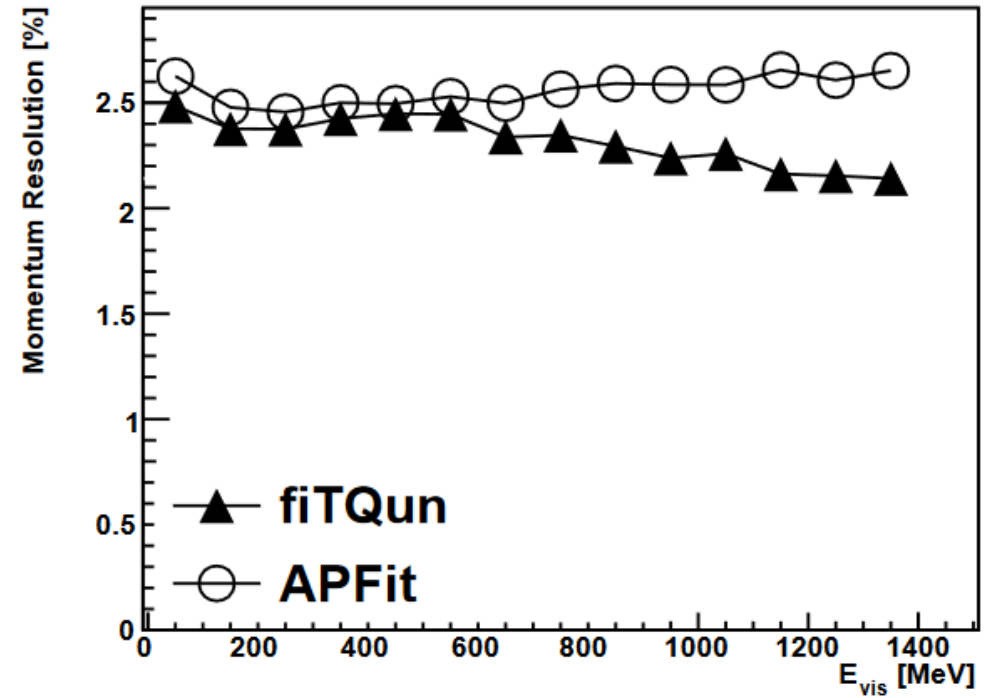
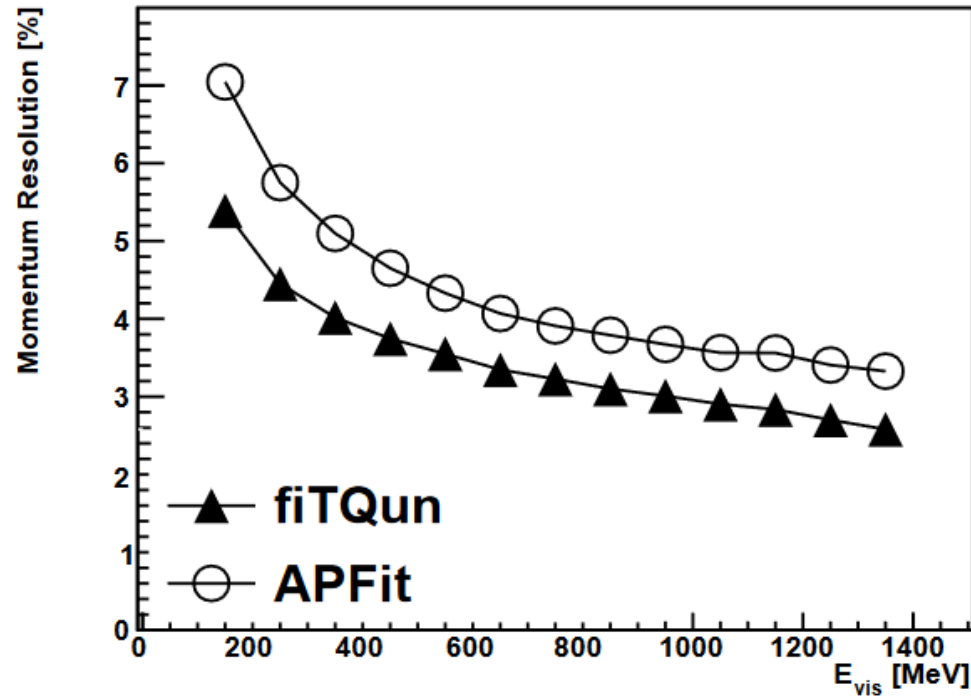


FIGURE 6.8: Single-ring electron (left) and muon (right) momentum resolution for FC CCQE events in atmospheric neutrino MC, compared between APFit (dashed line) and fiTQun (solid line). The bias (resolution) is defined as the mean (RMS) value of the ratio distribution between the reconstructed momentum and true momentum.

M. Jiang (2019), PhD Thesis, Kyoto University

Energy reconstruction SK/HK



M. Jiang (2019), PhD Thesis, Kyoto University

Beam oscillations for J-PARC to Hyper-K

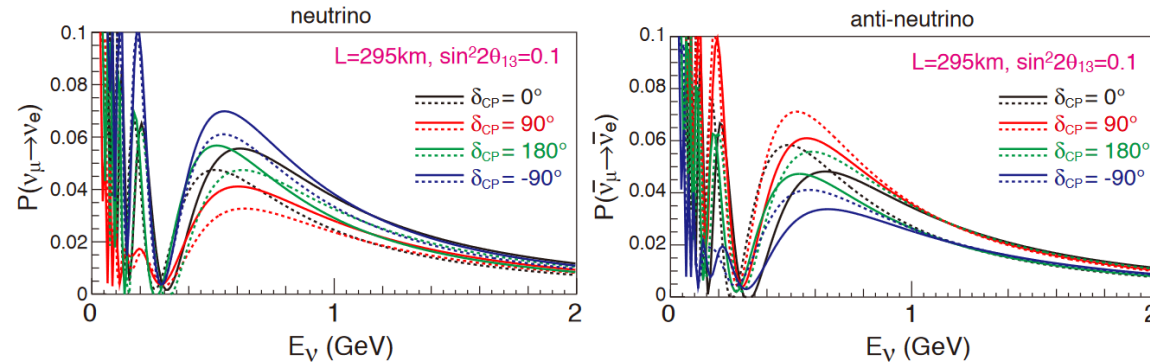
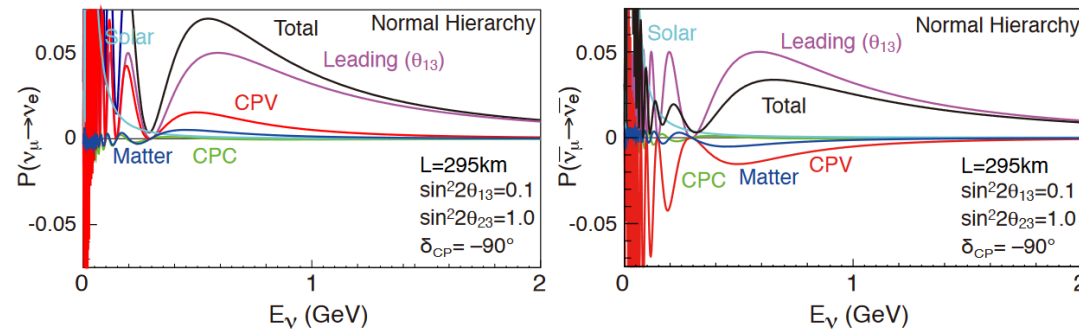
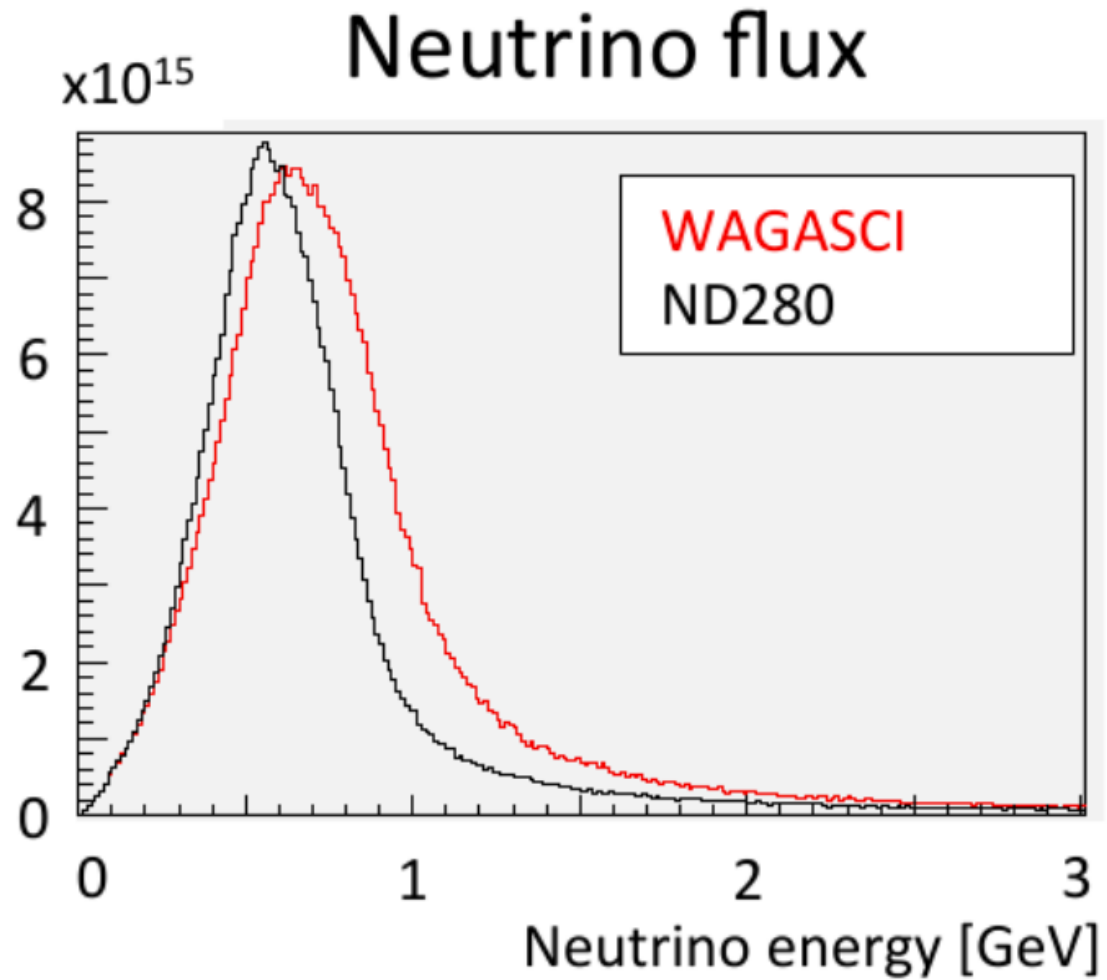


FIG. 129. Oscillation probabilities as a function of the neutrino energy for $\nu_\mu \rightarrow \nu_e$ (left) and $\bar{\nu}_\mu \rightarrow \bar{\nu}_e$ (right) transitions with $L=295$ km and $\sin^2 2\theta_{13} = 0.1$. Black, red, green, and blue lines correspond $\delta_{CP} = 0^\circ, 90^\circ, 180^\circ$ and -90° , respectively. Solid (dashed) line represents the case for a normal (invert) mass hierarchy.



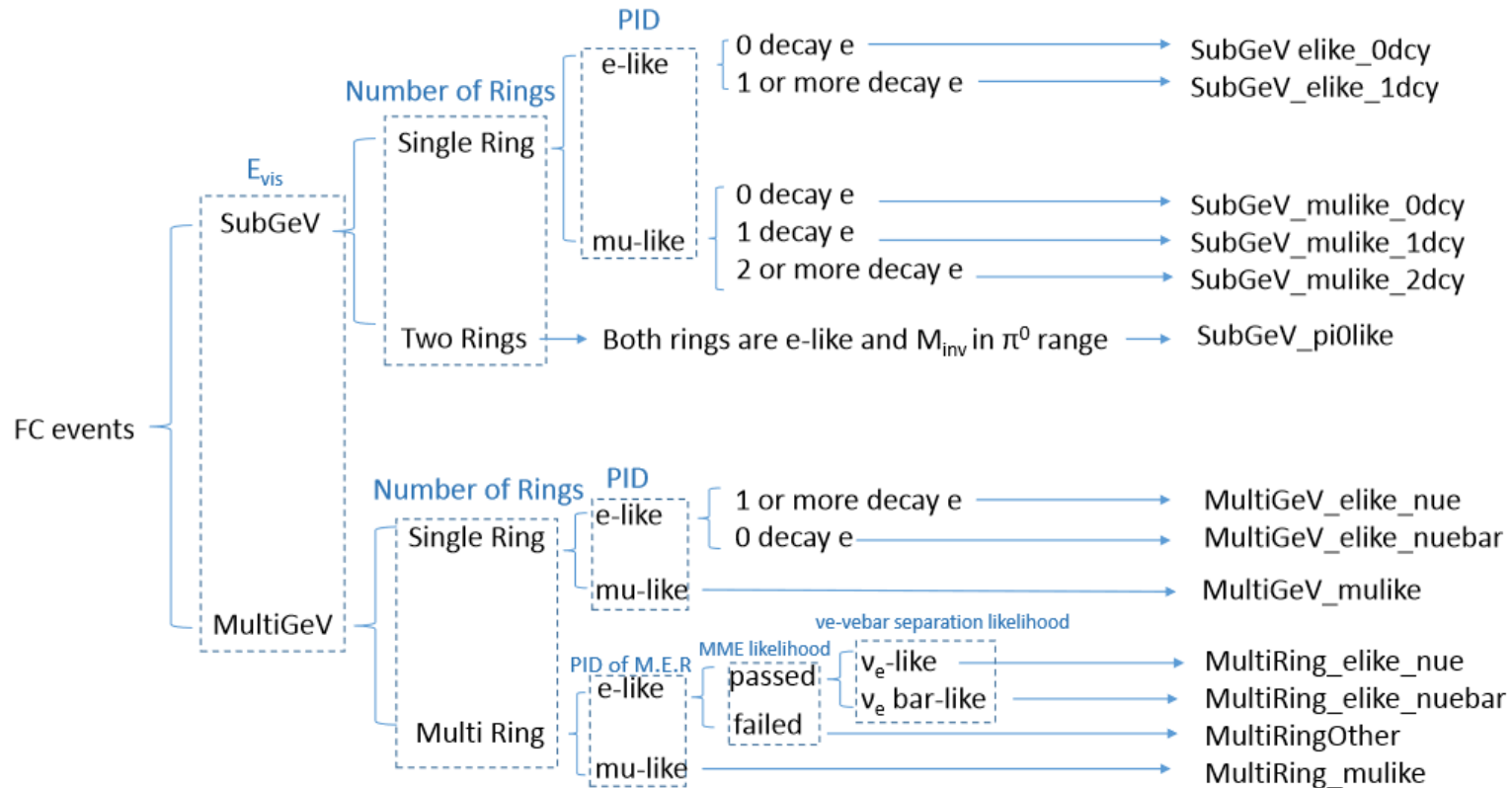
Hyper-K Design Report (2018)

T2K beam energies



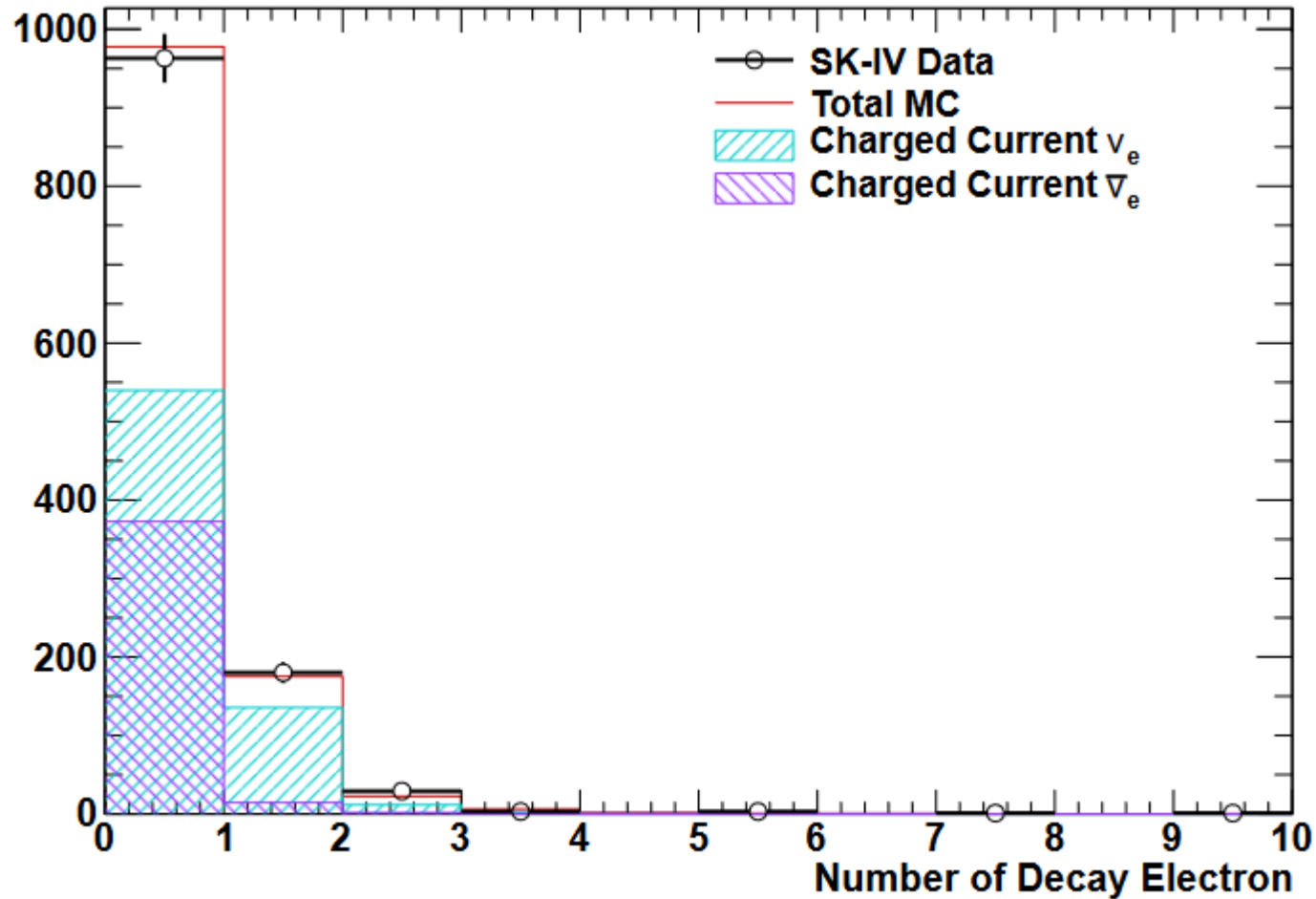
T. Ovsianikova et al. 2016 J. Phys.: Conf. Ser. 675 012030

Atmospheric ν event selection in SK



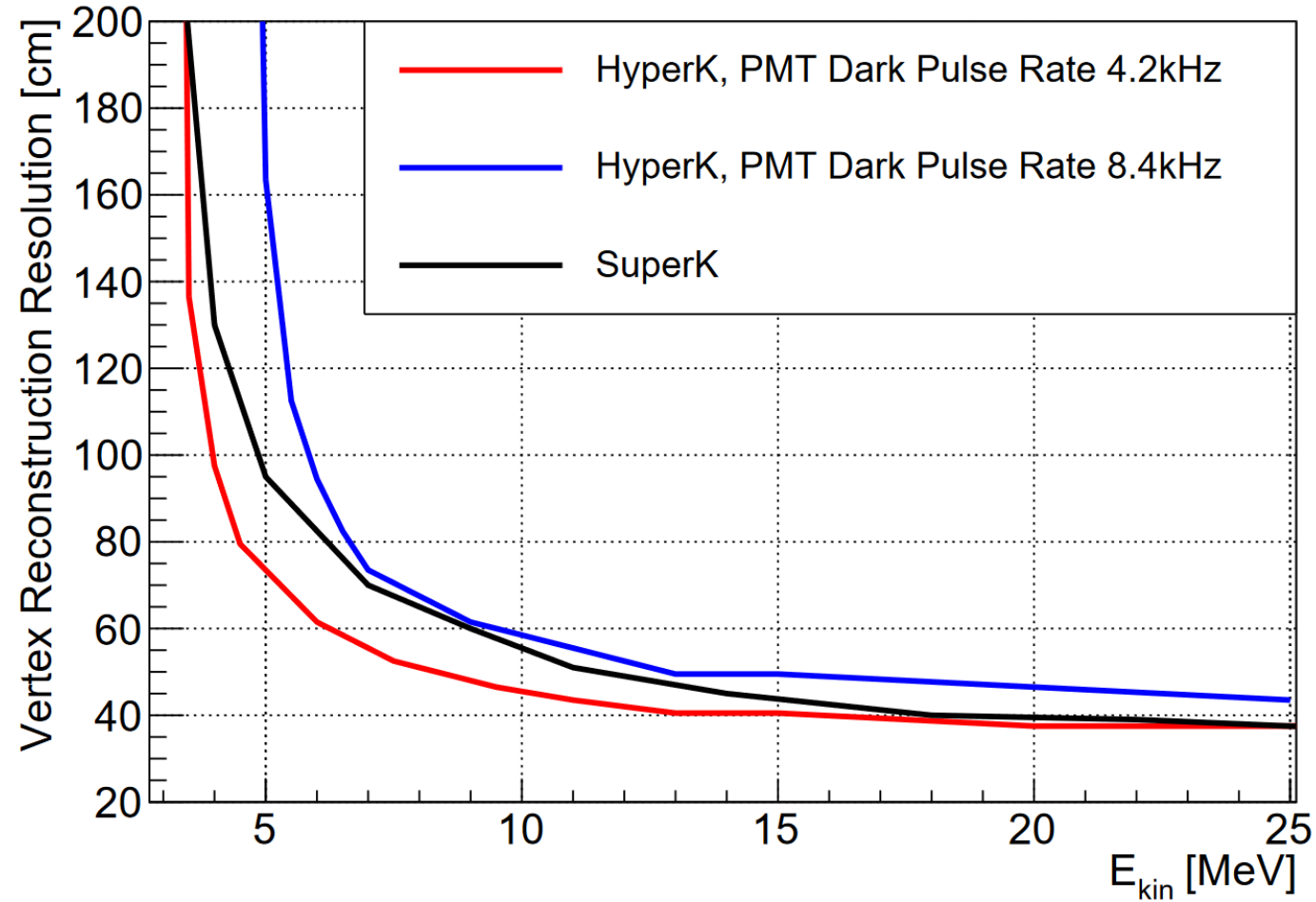
M. Jiang (2019), PhD Thesis, Kyoto University

Decay electrons for ν_e vs $\bar{\nu}_e$



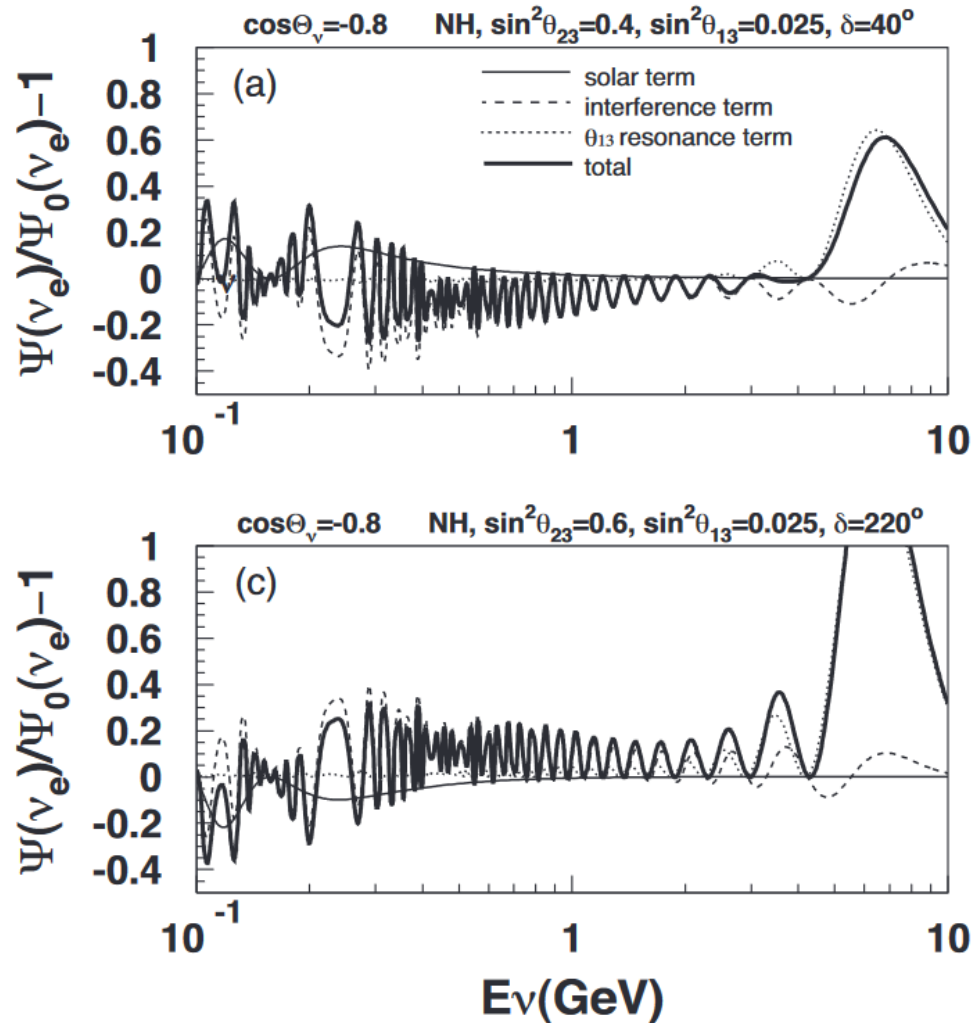
M. Jiang (2019), PhD Thesis, Kyoto University

Vertex reconstruction for BONSAI



Hyper-K Design Report (2018)

Effect of the θ_{23} octant for neutrino oscillations when $r \sim 2$

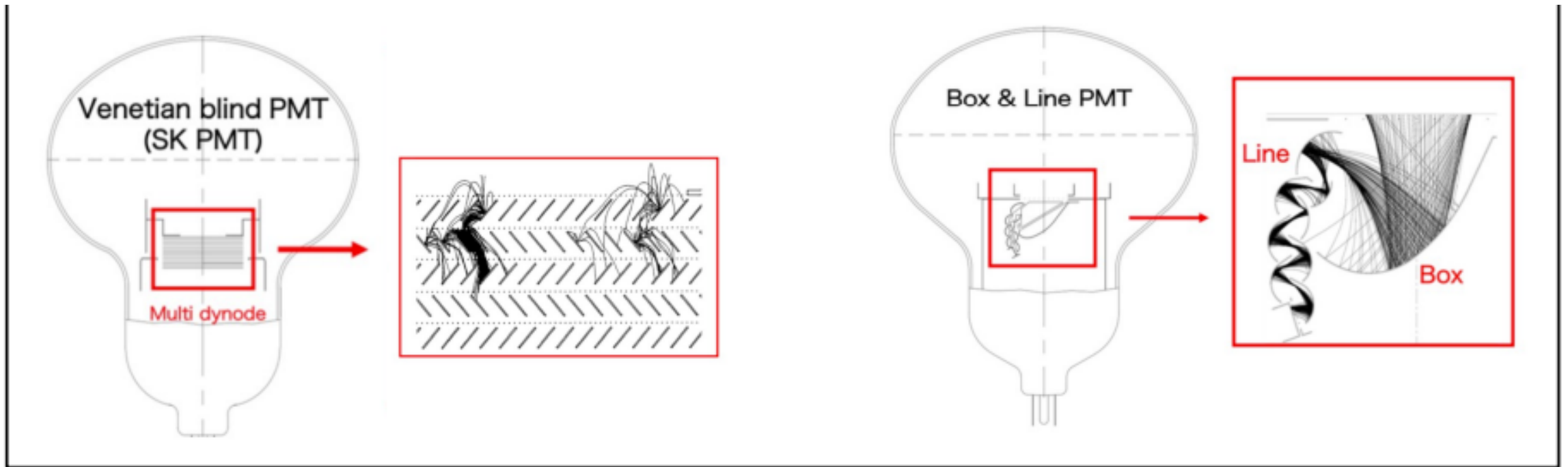


$$\frac{\Psi(\nu_e)}{\Psi_0(\nu_e)} - 1 \approx P_2 \cdot (r \cdot \cos^2 \theta_{23} - 1)$$

$$-r \cdot \sin \tilde{\theta}_{13} \cdot \cos^2 \tilde{\theta}_{13} \cdot \sin 2\theta_{23} \cdot (\cos \delta \cdot R_2 - \sin \delta \cdot I_2)$$

$$+ 2 \sin^2 \tilde{\theta}_{13} \cdot (r \cdot \sin^2 \theta_{23} - 1)$$

Gains in PMT performance for HK come from dynodes.



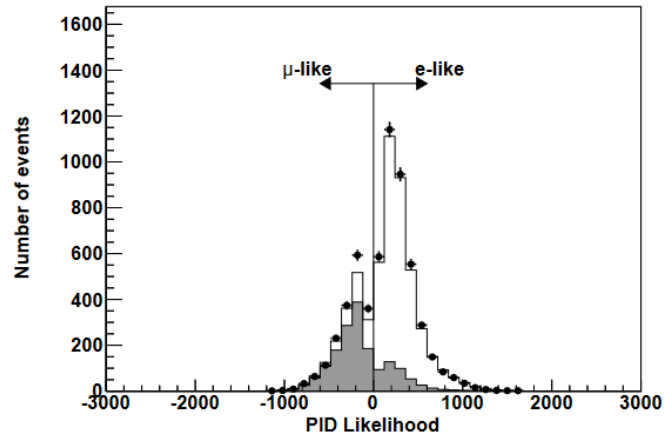
Slides C. Bronner (2018) workshop on new γ detectors

Ring reconstruction gets harder with multiple rings.

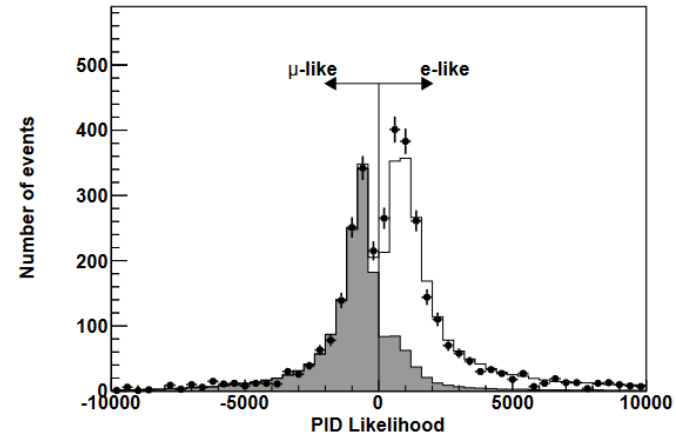
True Number of Rings	fitQun Reconstruction			APFit Reconstruction		
	1 ring	2 rings	≥ 3 rings	1 ring	2 rings	≥ 3 rings
True 1 ring	95.0%	4.64%	0.41%	95.9%	3.85%	0.29%
True 2 rings	27.8%	66.7%	5.56%	42.5%	52.8%	4.63%
True ≥ 3 rings	7.04%	25.5%	67.5%	20.2%	33.0%	46.8%

TABLE 6.2: Ring counting performance on FC atmospheric neutrino events. Both result of APFit and fitQun are shown here. The number of reconstructed rings are denoted by columns and the number of true rings are denoted by rows. The true rings are defined as only final state particles with energy 30 MeV higher than the Cherenkov threshold.

Ring reconstruction gets harder with multiple rings.



(a) Sub-GeV events



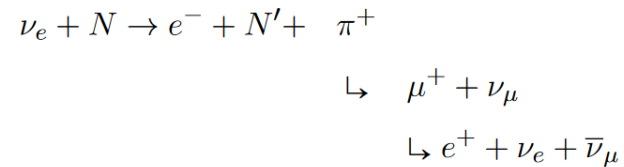
(b) Multi-GeV events

FIGURE 6.12: PID likelihood distributions of the most energetic ring for fully contained multi-ring events. Left figure shows the results of sub-GeV events while right figure are for multi-GeV events. Distribution for atmospheric neutrino data is denoted by the points and the MC prediction including neutrino oscillations is denoted by the histogram. The component of ν_μ charged-current interactions is shown by the shaded histogram. The statistical error are denoted by error bars. The reconstructed event vertex to the nearest ID wall (D_{wall}) is required to be larger than 200 cm.

M. Jiang (2019), PhD Thesis, Kyoto University

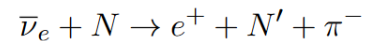
$\nu/\bar{\nu}$ separation for e -flavor

For CC ν_e interaction:



An decay electron (actually a positron) is produced finally.

For CC $\bar{\nu}_e$:



where π^- is more easy to be absorbed by oxygen nuclei and no decay electron is observed. Therefore multi-GeV single-ring e -like sample can be separated based the number of decay electrons as follows:

Number of decay electrons $> 0 \rightarrow \nu_e$ -like,

Number of decay electrons $= 0 \rightarrow \bar{\nu}_e$ -like.

M. Jiang (2019), PhD Thesis, Kyoto University